



## Geology and geochemistry of shallow drill cores from the Bosumtwi impact structure, Ghana

Daniel BOAMAH<sup>†</sup> and Christian KOEBERL<sup>\*</sup>

Department of Geological Sciences, University of Vienna, Althanstrasse 14, A-1090 Vienna, Austria

<sup>†</sup>Present address: Ghana Geological Survey Department, P.O. Box M80, Accra, Ghana

<sup>\*</sup>Corresponding author. E-mail: [christian.koerberl@univie.ac.at](mailto:christian.koerberl@univie.ac.at)

(Received 3 January 2003; revision accepted 2 August 2003)

**Abstract**—The 1.07 Ma well-preserved Bosumtwi impact structure in Ghana (10.5 km in diameter) formed in 2 Ga-old metamorphosed and crystalline rocks of the Birimian system. The interior of the structure is largely filled by the 8 km diameter Lake Bosumtwi, and the crater rim and region in the environs of the crater is covered by tropical rainforest, making geological studies rather difficult and restricted to road cuts and streams. In early 1999, we undertook a shallow drilling program to the north of the crater rim to determine the extent of the ejecta blanket around the crater and to obtain subsurface core samples for mineralogical, petrological, and geochemical studies of ejecta of the Bosumtwi impact structure. A variety of impactite lithologies are present, consisting of impact glass-rich suevite and several types of breccia: lithic breccia of single rock type, often grading into unbrecciated rock, with the rocks being shattered more or less in situ without much relative displacement (autochthonous?), and lithic polymict breccia that apparently do not contain any glassy material (allochthonous?). The suevite cores show that melt inclusions are present throughout the whole length of the cores in the form of vesicular glasses with no significant change of abundance with depth. Twenty samples from the 7 drill cores and 4 samples from recent road cuts in the structure were studied for their geochemical characteristics to accumulate a database for impact lithologies and their erosion products present at the Bosumtwi crater. Major and trace element analyses yielded compositions similar to those of the target rocks in the area (graywacke-phyllite, shale, and granite). Graywacke-phyllite and granite dikes seem to be important contributors to the compositions of the suevite and the road cut samples (fragmentary matrix), with a minor contribution of Papiakese granite. The results also provide information about the thickness of the fallout suevite in the northern part of the Bosumtwi structure, which was determined to be  $\leq 15$  m and to occupy an area of  $\sim 1.5$  km<sup>2</sup>. Present suevite distribution is likely to be caused by differential erosion and does not reflect the initial areal extent of the continuous Bosumtwi ejecta deposits. Our studies allow a comparison with the extent of the suevite at the Ries, another well-preserved impact structure.

### INTRODUCTION

Bosumtwi is one of only 18 currently confirmed African impact craters (Koeberl 1994; Master and Reimold 2000) and one of only 4 known impact craters associated with tektite strewn fields (Koeberl et al. 1997). The 1.07 Ma Bosumtwi crater (centered at 06°30' N and 01°25' W) is situated in the Ashanti region of Ghana, West Africa and is centered about 32 km from Kumasi, the regional capital. It is a well-preserved 10.5 km diameter complex impact structure that displays a pronounced rim and is almost completely filled by the 8 km diameter Lake Bosumtwi. The crater is excavated in 2 Ga-old metamorphosed and crystalline rocks of the Birimian system

(Junner 1937). The crater is surrounded by a slight near-circular depression and an outer ring of minor topographic highs with a diameter of  $\sim 20$  km (Jones et al. 1981; Garvin et al. 1992; Reimold et al. 1998; Wagner et al. 2002).

The origin of the Bosumtwi crater was controversial for a long time, as described by Junner (1937) and Jones (1985a). A volcanic origin for the crater was favored by early geologists, probably because impact craters were not fully appreciated at that time. Renewed interest in the 1960s led to the discovery of high-pressure silica polymorph coesite (Littler et al. 1961), Ni-rich iron spherules, and baddeleyite, the high-temperature decomposition product of zircon, in vesicular glass from suevite from the crater rim (El Goresy

1966; El Goresy et al. 1968), and shocked quartz (Chao 1968). These findings provided support for the impact hypothesis. Recently, further evidence of shock effects in the clasts in the suevites (Koeberl et al. 1998) has been described.

Substantial interest in the Bosumtwi crater has also come about from the studies of the Ivory Coast tektites, which were first reported by Lacroix (1934) from an area of about 40 km radius in Cote d'Ivoire, West Africa (Fig. 1a). Microtektites were found in deep-sea cores off the coast of Western Africa (Glass 1968, 1969) and have been related to the tektites found on land. As reviewed by, for example, Jones (1985a), Koeberl (1994), and Koeberl et al. (1997a, 1998), a variety of arguments have been used to conclude that the Bosumtwi

impact crater is the source of the tektites. These were based on the similarities in chemical and isotopic compositions, and identical ages for tektites and Bosumtwi impact glasses. According to Koeberl et al. (1998), the composition of the Ivory Coast tektites can be reproduced from a mixture of Bosumtwi country rocks that include about 70% phyllite-graywacke, 16% granite dike, and 14% Papiakese granite.

Research has intensified recently with regard to a number of aspects of the Bosumtwi crater. This includes studies of the petrology and geochemistry of the target rocks (Koeberl et al. 1998), structural analysis of the crater rim (Reimold et al. 1998), a high-resolution aerogeophysical survey including measurements of the total magnetic field, electromagnetic field, and gamma radiation measurements across the structure (Koeberl et al. 1997b; Ojamo et al. 1997; Pesonen et al. 1998, 1999; Plado et al. 2000), geochemistry of soils from the Bosumtwi structure (Boamah and Koeberl 2002), and a remote sensing investigation (Wagner et al. 2002). In addition, U. S. and German research teams are currently engaged in detailed land- and lake-based geophysical studies in the area (e.g., Scholz et al. 2002).

In this paper, we report on results obtained by shallow drilling outside the crater rim of Bosumtwi and by geochemical investigation on suevites and claystone (highly weathered target rocks) from those drill cores and on fragmentary matrix (micro-lithic breccia) from road cuts. The new geochemical data for the impact-produced breccias are compared to compositions of target or country rocks and Ivory Coast tektites and found to be in agreement with derivation of the breccias from the target rocks. Preliminary results of this study were reported in abstract form by Boamah and Koeberl (1999).

## GEOLOGY OF THE CRATER AREA

### Background

Detailed geological studies of the region around Lake Bosumtwi have been carried out since the 1930s (Junner 1937; Woodfield 1966; Moon and Mason 1967; Jones et al. 1981). More recent geological studies were carried out along a section across the western crater rim and on exposures in the sector around the northern and northeastern parts of the crater (Reimold et al. 1998). The region around Bosumtwi is largely covered by dense, tropical rainforest and shrubs. Thus, only studies of rare exposures along streams and road cuts are possible. Figure 1b schematically presents the geology around Lake Bosumtwi.

The Bosumtwi impact crater was excavated in lower greenschist facies metasediments of the 2.1–2.2 Ga Birimian Supergroup (cf., Wright et al. 1985; Leube et al. 1990). These supracrustals comprise interbedded phyllites and meta-tuffs together with meta-graywackes, quartzitic graywackes, shales, and slates. Birimian metavolcanic rocks (altered basic

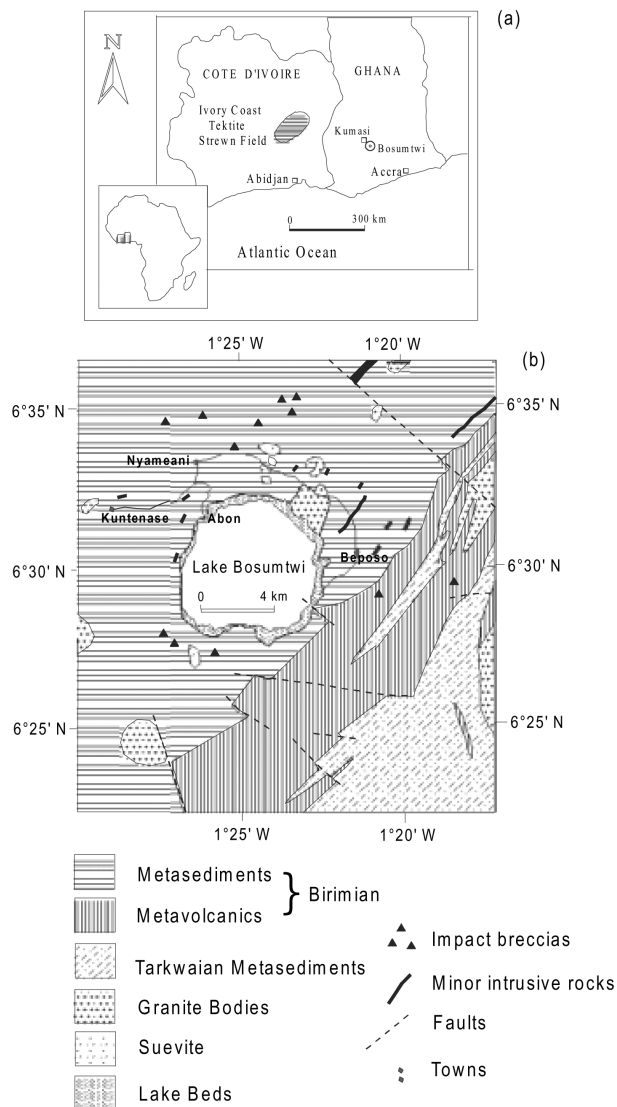


Fig. 1. a) Geographical location of the Bosumtwi impact crater, Ghana, in relation to the Ivory Coast tektite strewn field (after Koeberl et al. 1998); b) geological map of the area around Lake Bosumtwi, showing the provenance of different target rocks (after Jones et al. 1981; Reimold et al. 1998).

intrusives with some intercalated metasediments) reach out to the southeast of the crater. Tarkwaian clastic sedimentary rocks, which are regarded as the detritus of Birimian rocks (Leube et al. 1990), occur to the east and southeast of the crater. Recent rock formations include the Bosumtwi lake beds as well as soils and breccias associated with the formation of the crater (Junner 1937; Kolbe et al. 1967; Woodfield 1966; Moon and Mason 1967; Jones et al. 1981; Jones 1985b; Koeberl et al. 1997b; Reimold et al. 1998). Massive suevite deposits have been observed just outside the northern and southwestern crater rim (Fig. 1b).

### **Birimian Rocks**

Brecciated graywacke and phyllite dominate the geology of the study area, with a small number of strongly weathered dike- and pod-like granitoid intrusions (Junner 1937; Moon and Mason 1967; Reimold et al. 1998). Graywackes predominate and appear in many lithological variations between a silty, tuffaceous phyllite and tuffaceous grits. They are fine- to coarse-grained, light to dark gray, impure fragmental arenaceous rocks containing a mixture of clastic and tuffaceous material. The finer varieties exhibit good cleavage, but coarser types are more massive, and cleavage is often difficult to determine. The coarse-grained types grade into pebbly grits and conglomerates containing sub-angular to rounded pebbles of quartz and squeezed pebbles of phyllite and lava, and the fine-grained types grade into phyllites. The coarser types typically contain a high proportion of feldspar (feldspathic graywacke). Quartz veining and silicification are common in the graywacke. The graywackes observed in the road cuts are highly fractured and shattered.

The phyllites are gray to black, fine-grained rocks that are usually argillaceous but are tuffaceous in places. Some of the phyllites have been silicified and, generally, these silicified bands have been crumpled and sheared to a somewhat greater degree than the normal phyllites. Lenses and stringers of clear vein quartz occur within the foliae of both silicified and normal phyllites. These quartz veins are found in the same localities as the silicified phyllites and, for that reason, are considered to be of the same origin as the silicifying silica, but are slightly younger since veinlets of the clear quartz cut the silicified phyllite.

The Birimian metasediments have a general NE-SW strike and steep dips ( $\sim 80^\circ$ ) to either the northwest or the southeast. Around the crater rim, disturbances exist, resulting in irregular strikes and dips. These irregularities are believed to have been caused by the impact event that created the crater.

### **Intrusive Bodies**

Several Proterozoic granitic intrusions occur in the region around the crater (Fig. 1b), and some strongly weathered granitic dikes occur in the crater rim (Junner 1937;

Woodfield 1966; Moon and Mason 1967; Jones 1985a; Reimold et al. 1998). These granitic complexes and dikes probably belong to the Kumasi-type granitoid intrusions, for which an age of 2.0–2.1 Ga has been obtained (e.g., Taylor et al. 1992; Hirdes et al. 1992). In addition to granitoid dikes with, in places, granophyric texture (Reimold et al. 1998), some of these dikes appear aplitic in the field. Some of the granites are highly shattered and greatly weathered like those in the new road cuts from Asisiriwa towards Boamadumasi. Other granite outcrops include foliated types penetrated by small dikes of aplite and quartz veins. The foliations of the granite trend northeast, and the most prominent joints have a NW-SE direction. Most of the granitic dikes conform to the foliations or bedding planes of the Birimian rocks into which they are intruded. The Pekiakese granite complex to the northeast of the crater (Fig. 1b) is composed of a range of rock types, including hornblende diorite, biotite-muscovite granite, and an almost pure albite rock (Jones 1985b). Reimold et al. (1998) estimated the overall granitoid component in the region at no more than 2%. In addition, a few occurrences of dikes of dolerite, amphibolite, and intermediate rocks (minor intrusives) have been noted (Fig. 1b).

### **Impact Breccia**

Numerous breccia exposures have been mapped around the crater in the past (e.g., Junner 1937; Moon and Mason 1967; Woodfield 1966). However, whether all these breccias represent impact breccia is not certain. As pointed out by Reimold et al. (1998), at least some of the breccias, likely, are the results of lateritization and secondary mass-wasting processes in this tropical and topographically varied environment where weathering can attain thickness in excess of 50 m. The breccias at Bosumtwi could be grouped into 3 types based on composition and texture. These are: an autochthonous monomict breccia, a probably allochthonous polymict lithic breccia, and suevitic breccia.

A road cut at a recently constructed road in the north-northeast of the crater (Fig. 2), outside the crater rim (from Asisiriwa to Boamadumasi), shows an excellent exposure of partly consolidated breccia. This consists of unsorted angular fragments of graywacke ( $\sim 60\%$ ), phyllite ( $\sim 30\%$ ), schist ( $\sim 7\%$ ), and granite ( $\sim 3\%$ ) in a matrix of smaller fragments and dust derived from the same rocks. Most of the clasts are highly weathered and up to about 30 cm in size. Clast shapes range from angular to subrounded. Based on comparison with local weathering products (lateritic surfaces), this exposure, which is near drill hole BH6, is interpreted to represent a mixture of impact breccia and locally accumulated products of secondary mass-wasting processes along the steeply dipping outer rim slopes. Coarse pieces of quartz are rare, but fine-grained quartz occurs in the matrix. From the thickness of the road cut (about 2 m) and the core from the drill hole, the thickness of this impact breccia is estimated at more than 20 m. Similar

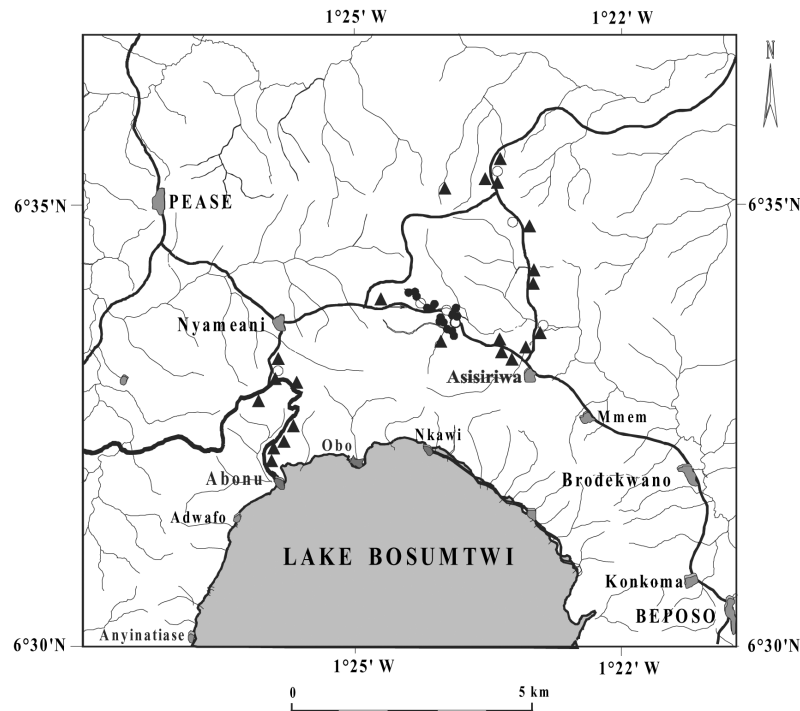


Fig. 2. Distribution of suevite deposits (solid circles) outside the crater rim to the north of the crater. The locations of the brecciated rocks examined, indicated by solid triangles, and the locations of the drill holes (open circles) are also shown.

breccias are exposed in nearby road cuts and along the new road from Boamadumasi toward Asisiriwa. Clast sizes are larger toward the Nyameani-Asisiriwa main road, up to 60 cm compared to around 30 cm in the breccias farther to the north from the crater towards Boamadumasi.

The monomict breccia often grades, on a meter scale, into unbrecciated rock. The rocks are shattered more or less in situ without much relative displacement. Shattered rocks consist of angular fragments of different sizes, which are irregularly distributed and recemented in a matrix of the same material. This type is found on the road from Nyameani to Asisiriwa and along the crater wall and was described by Moon and Mason (1967) as having formed by changes of the surface elevation without much lateral displacement.

Rarer is the Bosumtwi suevite, a glass-bearing breccia similar to the suevite of the Ries crater in Germany. The occurrence of suevite in the north and southwest of the Bosumtwi crater, outside the crater rim, was first mentioned by Junner (1937), who referred to the deposit as volcanic tuff and agglomerates. Suevite is defined (Stöffler and Grieve 1994) as polymict impact breccia including cogenetic impact melt particles, which are in a glassy or crystallized state, included in a clastic matrix containing lithic and mineral clasts in various stages of shock metamorphism. The Bosumtwi suevite is grayish in color with abundant glass and clasts up to about 40 cm in size.

The suevite is the most interesting deposit of the Bosumtwi crater formation. It represents that type of ejecta

formation that contains target rocks in all stages of shock metamorphism, including vitreous and devitrified impact glasses. The Bosumtwi suevite occurs as large blocks of up to several meters width and as patchy massive deposits more or less covered by thick vegetation in a marginal zone (~1.5 km<sup>2</sup>) outside the rim of the crater in the north, ~2.5 km from the lakeshore (location in the area of 1°23.5'–1°24.5' W and 6°33.5'–6°34.2' N). One of these outcrops is a massive suevite exposed for ~2 m in thickness. It contains melt inclusions and rock fragments (graywacke, phyllite, shale, granite) up to ~40 cm in size, with graywacke dominating. Most of the rock fragments are subangular in shape and less than 20 cm long and are arranged in a disordered fashion. Individual grains of quartz and feldspar are also present. The matrix is essentially composed of fine-grained particles of mainly quartz, feldspar, and highly vesicular glass.

#### THE 1999 SHALLOW DRILLING PROGRAM

In early 1999, a shallow drilling program was undertaken by the University of Vienna in cooperation with the Geological Survey Department of Ghana (GSD) using a skid-type rotary drill rig with 5 cm diameter core bits. Continuous core was retrieved in 1 m sections from each hole using a 1.5 m long, conventional core barrel. Seven holes were drilled to the north of the crater at a distance of 2.5 to 8 km from the lakeshore (locations in the area of 1°22'–1°27' W and 6°33'–6°36' N). Each hole was drilled to a maximum depth of about

30 m and core samples of impact breccias, suevites, and other rock types were recovered.

The drilling locations were chosen based on geophysical information obtained from an airborne radiometric map (equivalent concentrations of potassium and total radiation) produced by a high-resolution aerogeophysical survey across the Bosumtwi structure. The geophysical survey was undertaken by the Geological Survey of Finland in cooperation with the University of Vienna and the Geological Survey Department of Ghana (Koeberl et al. 1997b; Ojamo et al. 1997; Pesonen et al. 1998, 1999; Plado et al. 2000). The airborne radiometric map shows high concentrations of potassium around the crater and farther north where the drill holes were sited. The siting of the drill holes was also correlated with suevite outcrops from the geological map (Moon and Mason 1967) to recover a variety of impact lithologies, especially suevite.

The drill hole sites were individually chosen as the best available locations to recover specific lithologies relative to the goals of the drilling project. To the extent possible, drill holes were sited where the K concentrations were high. Fortunately, a new road was under construction crossing the area where the geophysical airborne radiometric highs occur in the north, and this road provided access to the drill sites BH4, BH5, and BH6. These sites are in lithic breccia terrain. Drill holes BH1 and BH3, on the other hand, were sited not very far from suevite outcrops with the aim of recovering suevite and determining the thickness of the fallout suevite deposit.

Geological mapping was also undertaken to help map the extent of the outcrops of various rock types and, especially, to identify the different types of impact breccia (Fig. 2). Because of the thick bush cover, bedrock and impact formations outside of the crater are only accessible along road cuts and in stream beds. Traverses were conducted along 4 road cuts, covering a total of about 30 km.

## SAMPLES AND ANALYTICAL METHODS

### Samples

Three groups of samples comprising 24 samples were selected for the present studies. These were obtained from the 7 drill cores (20 samples) and road cuts (4 samples). The first group of samples was matrix (groundmass) of the suevites. The matrix was selected to give relatively representative samples of the suevite for the geochemical studies. Eleven samples of this group were obtained from 2 cores, 5 from BH1 and 6 from BH3. Special attention was paid to avoid any clast over about 2 mm in diameter during the sampling processes. The second group of samples were classified as claystone. The third group comprises cemented small fragments (micro-lithic breccia), or fragmentary matrix (FM), sampled from road cuts. The sample locations are shown in Fig. 3. The sample numbers from the drill holes indicate the drill hole number and the depth in centimeters (i.e., BH1/1000

is a sample from drill hole BH1 taken from a depth of 1000 cm). Short petrographic descriptions of the rocks are summarized in Table 1.

### Analytical Methods

#### *XRF and INAA*

Major element oxides and some trace elements (Rb, Sr, Y, Zr, Nb, Co, Ni, Cu, Zn, V, Cr, and Ba) concentrations were determined on powdered samples by X-ray fluorescence (XRF) spectrometry at the Department of Geology, University of Witwatersrand, Johannesburg, South Africa. The details on procedures, precision, and accuracy are described by Reimold et al. (1994). Other trace elements (Sc, Cr, Co, Ni, Zn, As, Se, Br, Rb, Sr, Zr, Sb, Cs, Ba, Hf, Ta, W, Ir, Au, Th, and U) and the REEs were determined using instrumental neutron activation analysis (INAA). These analyses were carried out at the Institute of Geochemistry, University of Vienna, Austria. The quality of the analysis was monitored by the simultaneous analysis of the international geological reference materials (Govindaraju 1989). More details on analytical procedures are given in Koeberl (1993).

#### *X-Ray Diffractometry (XRD)*

Ten of the 24 samples were investigated using XRD techniques. Some samples were measured at the Department of Geology, University of Witwatersrand, South Africa and others at the Institute of Petrology, University of Vienna. The samples analyzed in South Africa were mainly suevite from drill hole BH1. These were BH1/0520, BH1/0950, BH1/1000, BH1/1300, BH1/1500, and one claystone (BH1/1600). Mineralogical analysis was done by Philips powder X-ray diffractometer (PW 1710), operating at 40 kV/20 mA and using Ni-filtered  $\text{CuK}\alpha$  radiation with a  $1^\circ$  divergent slit and on-line computer control. Diffractometer parameters were constant for all samples and measurements were made at 2-theta angles from  $3^\circ$  to  $70^\circ$ . Diffractograms were processed using PC-APD software.

The samples analyzed at the Institute of Petrology were BH3/0290, BH3/0990, BH1/1600, BH6/1850, and BD5. Mineralogical analysis was performed by a Philips powder X-ray diffractometer (PW 3710) operated at 45 kV/35 mA, using Ni-filtered  $\text{CuK}\alpha$  radiation, with automatic slit and online computer control. The samples were step-scanned from  $2^\circ$  to  $65^\circ$   $2\theta$ . Diffractograms were also processed using Philips PC-APD software.

## RESULTS AND DISCUSSION

### Drill Core Stratigraphy and Rock Types

The locations of the drill holes and the fragmentary matrix (micro-lithic breccia) from road cuts are shown in Fig. 3. Depending on the type of rocks, core recovery ranged from close to 80% (suevite) to 10% or less (lithic breccia and

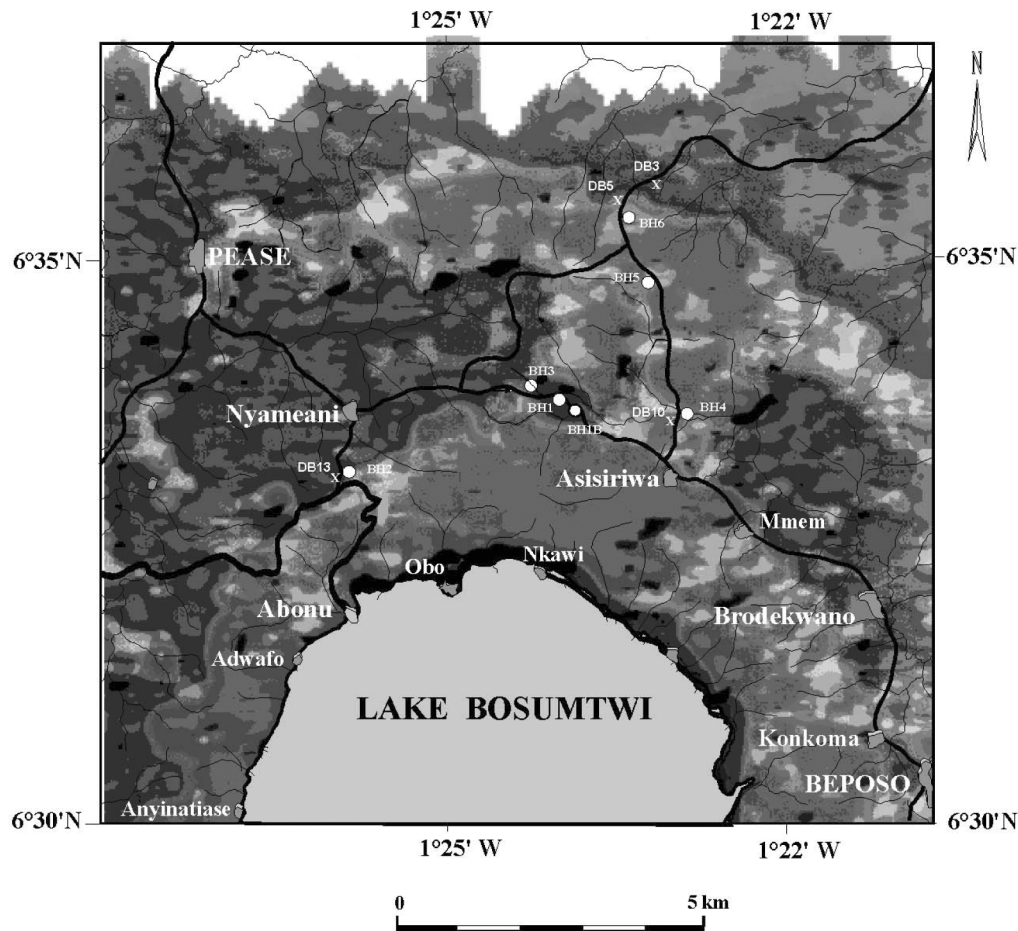


Fig. 3. Drill holes and road cut sample location map (overlay on radiometric map). The radiometric map (equivalent concentrations of potassium) was produced from a high resolution airborne geophysical survey carried out in the area (Ojamo et al. 1997).

weathered rocks). Suevite was encountered in 2 (BH1 and BH3) of the 7 holes at depths of 1.5–15.0 m and 2.0–10.0 m, respectively. Both of these holes terminated in highly weathered rocks (claystone). Descriptions of the suevite cores are given in the Appendix; for descriptions of the other cores, contact the authors. The dominant rocks from the lithic breccia locations (BH1B, BH2, BH4, BH5, and BH6) are graywacke and phyllite with minor shale, schist, and granite. The stratigraphic columns of these cores are shown in Fig. 4, together with the locations sampled for this study.

In hand specimen, all suevite samples from the 2 drill holes resemble each other. The samples are generally grayish in color. Impact glasses in various size ranges, from microscopic particles to fragments about 20 cm across, are found within the suevite. Graywacke and phyllite dominate the rock clast population, besides rare granite. The clasts range from a few mm to tens of cm in length and are angular to subrounded. The rock fragments and larger glass bodies are irregularly distributed into a matrix consisting of small glass particles, mineral fragments (mostly quartz and feldspar), and clay. The constituents of the suevite show all degrees of shock metamorphism (e.g., PDF, diaplectic glass, ballen-quartz, and

fused or melted minerals and rocks), but the most characteristic of the suevite are inclusions of very friable and porous, dark greenish-brown material which represents recrystallized, highly vesicular glass produced by shock fusion of target rocks.

Macroscopic studies of the recovered suevite cores show that the distribution of melt inclusions (in the form of vesicular glasses) does not change throughout the whole length of the cores (Fig. 5). Glasses are irregular in shape, with some of them showing flow bands. In general, the groundmass or matrix occupies about 75 vol% of the suevite, glass melt is about 15 vol%, rock fragments (graywacke, phyllite, shale, schist, and granite) are about 10 vol%, and mineral clasts (quartz and feldspar) are less than 1 vol%. This agrees well with recent measurements by Koeberl et al. (2002) based on high resolution X-ray computed tomography. Matrix was taken as materials less than about 1 mm in size. Most fragments are less than 20 mm in diameter, but a few are larger than the core diameter (5 cm). Because the vertical sections of the suevite revealed no primary variation in composition or grain size, the process of deposition is assumed to have been uniform and of short duration. Figure 5

Table 1. Description of samples analyzed in this study.

Sample number	Location	Description
BH1/0520	Drill hole 1: 6°33.9' N, 1°23.9' W	Altered suevite; greenish-gray in color with dark gray to greenish-black glassy inclusions and light-colored, granitoid-derived lithic and mineral clasts, in addition to metasediment clasts less than 2 mm in size.
BH1/0950	"	Altered suevite; similar to above.
BH1/1000	"	Altered suevite; greenish-gray in color with altered yellowish clast suspected to be dolerite.
BH1/1300	"	Altered suevite; greenish-gray in color with inclusions of vesicular glass fragments and clasts of phyllite, graywacke, and granitoids less than 2 mm in size.
BH1/1500	"	Suevite; similar to above but more altered, with some clay.
BH1/1600	"	Claystone (highly weathered or decomposed target rock).
BH1B/0600	Drill hole 1B: 6°33.8' N, 1°23.8' W	Claystone (highly weathered or decomposed target rock).
BH2/0950	Drill hole 2: 6°33.4' N, 1°25.9' W	Claystone (highly weathered or decomposed target rock).
BH2/1800	"	Claystone (highly weathered or decomposed target rock).
BH3/0220	Drill hole 3: 6°34' N, 1°24.1' W	Altered suevite; greenish-gray in color with inclusions of vesicular glass fragments and clasts of phyllite, graywacke, and granitoid-derived lithic and minerals less than 2 mm in size.
BH3/0290	"	Altered suevite; similar to above but with abundant vesicular glass inclusions.
BH3/0615	"	Altered suevite; grayish in color with inclusions of glass particles and clasts of vesicular glass, quartz, feldspar and graywacke less than 2 mm.
BH3/0660	"	Altered suevite; similar to above with dark brown materials in cracks of the broken pieces.
BH3/0865	"	Altered suevite; greenish-gray in color with inclusions of vesicular glass fragments and some light colored materials (quartz and feldspar) and clasts of phyllite, graywacke, and granitoids.
BH3/0990	"	Altered suevite; similar to above.
BH4/0450	Drill hole 4: 6°33.9' N, 1°22.8' W	Claystone (highly weathered or decomposed target rock).
BH4/1350	"	Claystone (highly weathered or decomposed target rock).
BH5/0650	Drill hole 5: 6°35' N, 1°23.1' W	Claystone (highly weathered or decomposed target rock).
BH6/1850	Drill hole 6: 6°35.7' N, 1°23.3' W	Claystone (highly weathered or decomposed target rock).
BH6/2100	"	Claystone (highly weathered or decomposed target rock).
BD3	Road cut: 6°35.7' N, 1°23.3' W	Cemented small fragments; grayish-brown in color, composed of clay and fine clasts of phyllite, graywacke, and granite.
BD5	Road cut: 6°35.7' N, 1°23.3' W	Fragmentary matrix; grayish-brown in color, composed of clay and fine particles and clasts of phyllite, graywacke, and granite.
BD10	Road cut: 6°33.8' N, 1°22.9' W	Fragmentary matrix; composed of clay with fine clasts of granite, graywacke, and phyllite.
BD13	Road cut: 6°33.3' N, 1°25.9' W	Fragmentary matrix; composed of clay with fine particles of graywacke, granite, and phyllite.

shows schematic stratigraphic columns of the 2 drill holes through suevite and the sampling locations.

### Shock Metamorphism at the Bosumtwi Structure

Shock metamorphism provides unambiguous evidence for conditions uniquely associated with impact cratering (see, e.g., Stöffler and Langenhorst 1994; Koeberl 1997; French 1998, and references therein). Distinctive shock metamorphic effects at Bosumtwi have so far been found only in the suevites, which occur outside of the crater rim and which represent ejecta from the lower part of the crater. None of the fractured and shattered metasediments and granites display any evidence of characteristic shock effects (Koeberl et al. 1998). Shock metamorphic effects in rocks from the Bosumtwi crater were first mentioned by Littler et al. (1961) and Chao (1968), who described the presence of coesite and shocked minerals in suevite from outside the crater rim.

Microscopic study of thin sections from the suevites shows many typical shock-induced metamorphic textures. Shock-induced planar deformation features (PDFs), as well as other types of planar deformations, are seen in both quartz and feldspar. Biotite grains are strongly kinked. Partly vesicular glassy fragments, in different stages of devitrification, are common in the suevites, as are crystals of quartz and feldspar showing different stages of isotropization and melting, together with apparently undeformed rock and crystal fragments. Diaplectic quartz and feldspar glasses are also present. A few of the quartz and diaplectic quartz glass particles that occur isolated in the matrix melt have been altered by high temperatures. Transformation of quartz to cristobalite and subsequent reversion to quartz is indicated by particles showing the typical "ballen" structure (Carstens 1975), which consists of microcrystalline quartz.

All suevite glasses are more or less devitrified, i.e., crystallized below the glass-transition temperature, usually

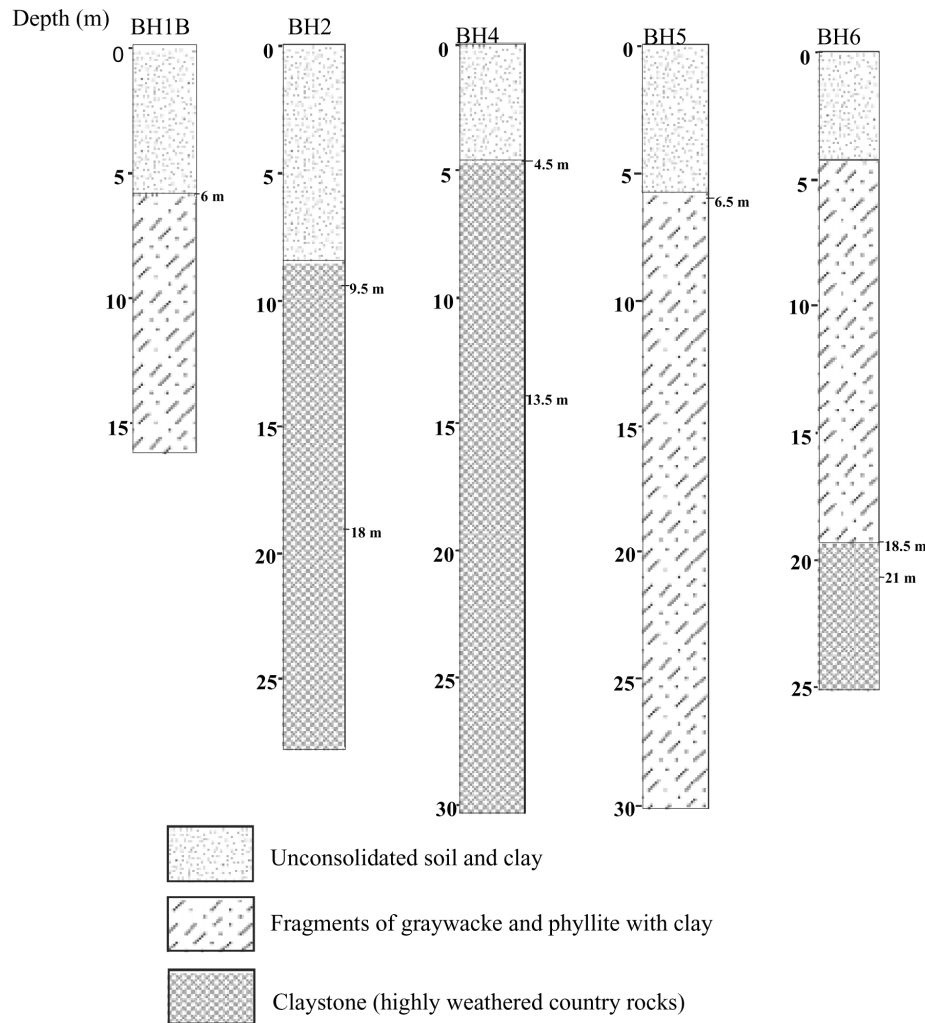


Fig. 4. Stratigraphic column of drill cores BH1B (drilled to 16 m), BH2 (drilled to 28 m), BH4 (drilled to 30.5 m), BH5 (drilled to 30 m), and BH6 (drilled to 25 m). The sample locations for geochemical studies are indicated in the right margins.

occurring by the formation of alkali feldspar spherulites (Carstens 1975). Crystallites are very fine and are represented by laths of feldspar and mostly pyroxene. By petrographic and microprobe analysis (Boamah et al., in preparation), plagioclase and pyroxenes have been identified as the main devitrification products. Details of the petrographical studies, including shock petrography, will be presented elsewhere.

### Mineralogical Observations

The XRD results show that quartz dominates in all the samples, with albite and montmorillonite (altered from the glass in the suevite) being present in the suevites as well. Muscovite and kaolinite also occur in the highly weathered suevite sample BH1/1500, which contains a significant amount of clay. Kaolinite is present in the highly weathered samples (claystone) and the cemented small fragments. The claystone and the fragmentary matrix samples have a mixed layer of clay and albite in addition to quartz.

### Geochemistry

Results of the major and trace element analyses, together with some characteristic geochemical ratios, of 24 samples comprising 11 suevite, 4 fragmentary matrix, and 9 claystone samples are given in Tables 2 and 3. For comparison purposes, mean compositions calculated for the various groups of samples, together with those of the target rocks and tektites (Koeberl et al. 1998), and upper continental crust (Taylor and McLennan 1985) are reported in Table 4.

#### Major Element Distributions

The three groups of samples (suevite, fragmentary matrix, and claystone) show compositions that have little variation within the groups (Tables 2 and 3) but significant differences between groups, especially for CaO and Na<sub>2</sub>O contents. The most significant variation is observed for the claystone samples, which may be attributed to intense

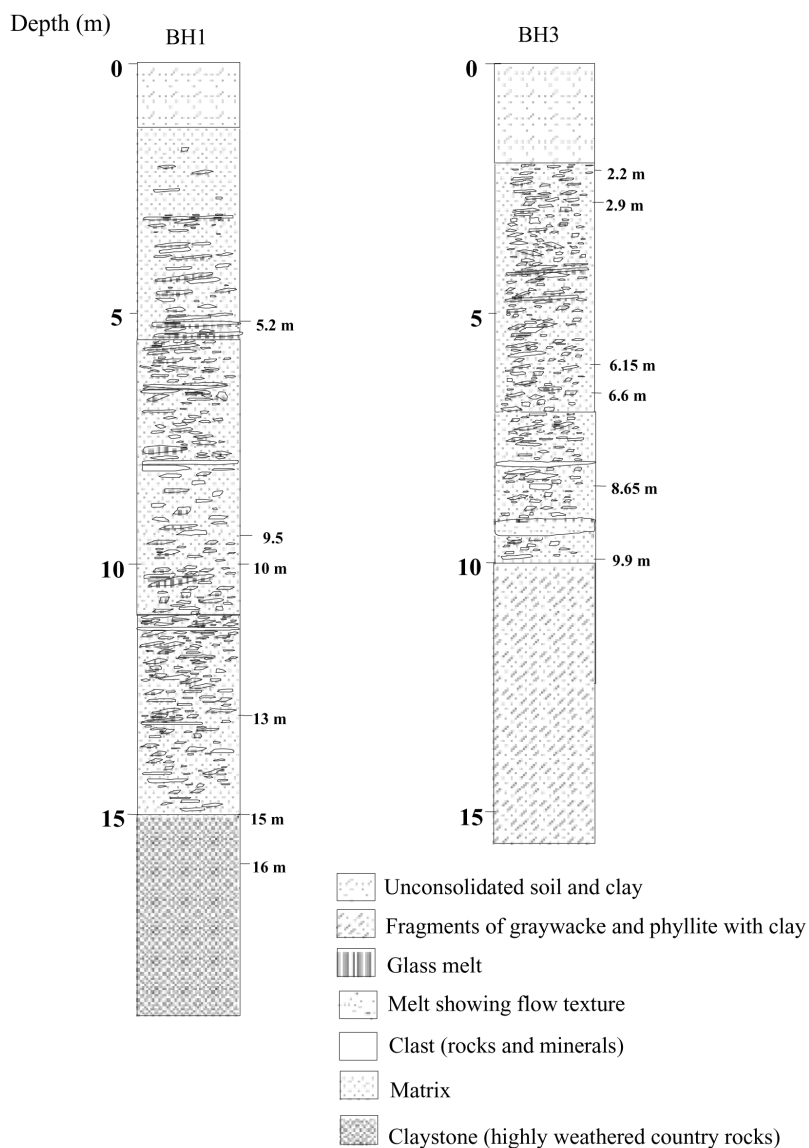


Fig. 5. Stratigraphic column for the 2 drill holes through suevite: drill cores BH1 (drilled to 19 m) and BH3 (drilled to 16 m). In BH1, suevite is between 1.5 m and 15 m (thickness of about 13 m), while in BH3, it is between 2 m and 10 m (thickness of about 8 m). The sample locations for geochemical studies are indicated in the right margins.

weathering with the subsequent leaching of these elements from the weathered samples. Compared to the suevite samples, the claystone (highly weathered target rocks) and the fragmentary matrix samples are relatively lower in CaO content. The relatively higher CaO content in the suevite is suggestive of a carbonate component, as fillings in the voids in the suevite (Boamah et al., in preparation). There have been similar observations in suevite from the Ries impact structure (e.g., Engelhardt 1972) that were associated with the presence of secondary carbonate precipitated from cool weathering solutions. The  $\text{Al}_2\text{O}_3$  content is probably indicative of a clay component in the rocks as indicated by the XRD measurements. Since CaO,  $\text{Na}_2\text{O}$ ,  $\text{K}_2\text{O}$ , and MgO are highly susceptible to alteration during weathering, hydrothermal

activity, or metamorphism (Gibbs et al. 1986), we cannot demonstrate rigorously whether these processes or variations in provenance account for variations in these elements.

Table 2 makes it evident that the compositions of the suevites from the 2 drill holes do not change significantly with depth. The average compositions of suevite of BH1 are, however, slightly more mafic than those of BH3. For example, concentrations of  $\text{Fe}_2\text{O}_3$  and MgO average 7.5 wt% and 1.81 wt% ( $n = 5$ ), respectively, in BH1, compared with 5.8 wt% and 1.25 wt% ( $n = 6$ ), respectively, in BH3. Other differences occur, but because of the small number of samples and the range in composition of the samples, these differences may not be significant. Sample BH1/1000 has the lowest  $\text{SiO}_2$  content (55.42 wt%) among the suevite and fragmentary

Table 2. Chemical composition of suevite from 2 drill holes (BH1 and BH3) from the Bosumtwi area.<sup>a</sup>

	Suevite, BH1					Suevite, BH3						Suevite, average	
	BH1/ 0520	BH1/ 0950	BH1/ 1000	BH1/ 1300	BH1/ 1500	BH3/ 0220	BH3/ 0290	BH3/ 0615	BH3/ 0660	BH3/ 0865	BH3/ 0990	BH1	BH3
SiO <sub>2</sub>	64.74	64.94	55.42	64.44	61.18	65.15	64.06	65.73	65.96	63.17	64.63	62.14	64.78
TiO <sub>2</sub>	0.61	0.61	0.83	0.67	0.67	0.56	0.67	0.60	0.61	0.62	0.59	0.68	0.61
Al <sub>2</sub> O <sub>3</sub>	16.20	15.81	12.78	16.15	17.05	14.87	15.84	15.60	16.34	14.64	16.15	15.60	15.57
Fe <sub>2</sub> O <sub>3</sub>	5.99	6.41	13.14	5.59	6.36	6.11	5.85	5.78	5.39	6.88	4.91	7.50	5.82
MnO	0.08	0.08	0.10	0.14	0.19	0.04	0.06	0.14	0.10	0.19	0.10	0.12	0.11
MgO	1.87	1.42	2.81	1.63	1.34	0.92	0.95	1.02	1.07	1.27	1.45	1.81	1.11
CaO	1.87	1.85	1.61	2.24	0.29	0.42	1.84	1.08	1.58	1.19	1.36	1.57	1.25
Na <sub>2</sub> O	2.28	2.47	1.39	2.12	0.79	1.41	1.91	1.92	2.05	1.62	1.02	1.81	1.66
K <sub>2</sub> O	1.89	1.83	0.78	1.60	0.97	0.89	1.15	1.29	1.46	0.97	1.18	1.41	1.16
P <sub>2</sub> O <sub>5</sub>	0.11	0.12	0.12	0.12	0.05	0.04	0.09	0.06	0.09	0.08	0.08	0.10	0.07
LOI	4.86	4.92	11.19	5.76	10.41	9.07	7.12	7.17	5.76	9.21	9.01	7.43	7.89
Total	100.51	100.45	100.18	100.48	99.31	99.49	99.54	100.40	100.42	99.84	100.47	100.19	100.03
Sc	13.7	14.4	30.9	13.8	15.6	11.4	14.9	14.8	12.6	14.3	11.7	17.7	13.3
V	106	106	249	98	138	92	96	114	109	118	93	139	104
Cr	175	167	2229	213	166	175	210	186	173	181	233	590	193
Co	18.4	17.5	56.6	14.6	23.3	16.5	15.6	14.5	12.6	19.8	9.62	26.1	14.8
Ni	64	75	423	65	148	69	71	64	52	79	55	155	65
Cu	17	21	86	17	21	17	19	20	15	22	5	32	16
Zn	76	77	117	61	64	64	69	67	72	76	60	79	68
As	4.75	4.20	4.71	2.89	2.89	2.65	2.74	2.19	3.09	2.26	1.77	3.89	2.45
Se	0.07	<0.13	<0.21	0.06	0.07	0.18	0.03	0.03	0.16	0.17	<0.11	0.07	0.11
Br	0.23	0.18	0.23	0.21	0.20	0.25	0.16	0.24	0.21	0.18	0.24	0.21	0.21
Rb	71.2	69.0	23.2	64.3	70.4	21.1	43.5	46.4	60.1	45.1	51.1	59.6	44.6
Sr	338	342	322	330	169	219	327	316	352	297	302	300	302
Y	19	17	15	15	18	18	15	17	15	15	13	17	16
Zr	128	126	68	131	137	119	136	115	134	121	129	118	126
Nb	8	8	7	9	9	8	9	8	8	8	8	8	8
Sb	0.33	0.09	0.52	0.34	0.62	0.20	0.44	0.26	0.31	0.42	0.15	0.38	0.30
Cs	3.39	2.81	1.35	2.81	14.9	1.11	2.77	2.83	3.33	2.51	2.97	5.05	2.59
Ba	684	659	379	541	520	516	617	557	576	521	619	557	568
La	22.0	18.2	10.0	18.8	22.2	29.8	20.8	19.1	17.2	16.7	12.8	18.2	19.4
Ce	42.3	38.9	22.9	41.4	46.6	52.0	45.8	38.4	35.7	36.0	26.2	38.4	39.0
Nd	23.2	16.5	10.5	17.0	24.3	25.2	19.9	20.1	16.2	15.3	12.0	18.3	18.1
Sm	4.55	3.58	2.72	3.67	4.34	4.38	3.53	3.87	2.87	3.10	2.23	3.77	3.33
Eu	1.30	1.10	0.73	1.10	1.25	1.10	1.27	1.06	1.00	1.02	0.79	1.10	1.04
Gd	3.72	4.10	2.03	3.43	2.78	3.52	3.09	2.84	0.62	3.32	2.68	3.21	2.68
Tb	0.67	0.53	0.37	0.45	0.54	0.51	0.47	0.50	0.32	0.44	0.36	0.51	0.43
Tm	0.26	0.26	0.66	0.23	0.33	0.31	0.20	0.44	0.21	0.31	0.38	0.35	0.31
Yb	1.92	1.50	1.73	1.44	1.96	1.78	1.35	1.87	1.20	1.35	1.22	1.71	1.46
Lu	0.24	0.22	0.27	0.20	0.30	0.24	0.22	0.27	0.17	0.21	0.19	0.25	0.22
Hf	3.61	3.34	2.78	3.40	3.29	3.16	3.42	3.28	3.14	2.85	3.14	3.28	3.17
Ta	0.35	0.38	0.12	0.30	0.42	0.23	0.31	0.30	0.29	0.30	0.31	0.31	0.29
Ir (ppb)	0.9	<2.8	<7.2	<2.6	<2.3	<2.7	<3	<2.3	1.3	<2.9	<2.6	–	–
Au (ppb)	5.8	1.6	18.8	39.9	6.5	8.4	4.7	7.5	5.6	2.2	12.5	14.5	6.8
Th	3.28	3.15	1.24	3.44	3.38	2.83	3.37	2.88	2.84	2.94	3.02	2.90	2.98
U	0.84	0.82	0.86	1.43	2.59	0.40	1.23	1.08	0.76	0.84	0.74	1.31	0.84
CIA	64	63	68	63	86	79	67	71	68	71	75	69	72
K/U	15683	15185	6472	13277	8049	7385	9543	10704	12115	8048	9791	11733	9598
Zr/Hf	35.5	37.7	24.5	38.5	41.6	37.7	39.8	35.1	42.7	42.5	41.1	35.6	39.8
La/Th	6.71	5.78	8.06	5.47	6.57	10.5	6.17	6.63	6.06	5.68	4.24	6.52	6.55
Hf/Ta	10.3	8.79	23.2	11.3	7.83	13.7	11.0	10.9	10.8	9.50	10.1	12.3	11.0
Th/U	3.90	3.84	1.44	2.41	1.31	7.08	2.74	2.67	3.74	3.50	4.08	2.58	3.97
La <sub>N</sub> /Yb <sub>N</sub>	7.74	8.20	3.91	8.82	7.65	11.3	10.4	6.90	9.69	8.36	7.09	7.26	8.96
Gd <sub>N</sub> /Yb <sub>N</sub>	1.57	2.22	0.95	1.93	1.15	1.60	1.86	1.23	0.42	1.99	1.78	1.56	1.48
Eu/Eu*	0.97	0.88	0.95	0.95	1.10	0.86	1.18	0.98	2.29	0.97	0.99	0.97	1.21

<sup>a</sup>Major elements in wt%, trace elements in ppm, except as noted. Total Fe as Fe<sub>2</sub>O<sub>3</sub>. Eu/Eu\* = Eu<sub>N</sub>/(Sm<sub>N</sub> × Gd<sub>N</sub>)<sup>0.5</sup>. Chemical index of alteration (CIA) = (Al<sub>2</sub>O<sub>3</sub>/[Al<sub>2</sub>O<sub>3</sub> + CaO + Na<sub>2</sub>O + K<sub>2</sub>O]) × 100 in molecular proportions.

Table 3. Chemical composition of fragmental breccia matrix and clay (weathered target rocks) from Bosumtwi.<sup>a</sup>

	Claystone					Fragmentary matrix							
	BH1/ 1600	BH1B/ 0600	BH2/ 0950	BH2/ 1800	BH4/ 0450	BH4/ 1350	BH5/ 0650	BH6/ 1850	BH6/ 2100	BD3	BD5	BD10	BD13
SiO <sub>2</sub>	64.57	62.93	57.10	68.69	72.61	59.67	53.77	60.01	62.35	65.28	68.09	63.37	64.69
TiO <sub>2</sub>	0.60	0.65	0.76	0.56	0.49	0.68	0.86	0.76	0.74	0.62	0.54	0.57	0.64
Al <sub>2</sub> O <sub>3</sub>	17.48	16.89	22.24	17.17	14.69	17.61	21.34	18.28	19.25	16.80	15.26	17.57	17.46
Fe <sub>2</sub> O <sub>3</sub>	5.71	6.48	8.07	5.08	3.75	9.28	8.64	7.38	5.24	6.11	4.97	6.33	6.47
MnO	0.10	0.10	0.10	0.13	0.03	0.03	0.00	0.06	0.02	0.05	0.05	0.05	0.07
MgO	1.28	2.15	0.46	0.68	1.14	2.05	2.28	1.97	1.56	1.75	1.68	1.30	1.19
CaO	0.11	0.58	0.01	0.02	0.17	0.29	0.17	0.30	0.26	0.03	0.20	0.25	0.00
Na <sub>2</sub> O	0.41	1.25	0.46	0.42	1.33	1.04	0.43	0.63	0.60	1.11	3.03	2.97	0.55
K <sub>2</sub> O	2.27	2.74	0.78	1.41	0.96	2.24	3.93	2.29	2.26	1.91	1.42	1.99	1.94
P <sub>2</sub> O <sub>5</sub>	0.09	0.13	0.03	0.06	0.04	0.11	0.11	0.04	0.04	0.05	0.03	0.06	0.05
LOI	6.97	6.09	9.48	6.57	5.11	7.38	7.95	8.73	8.08	6.46	5.13	5.92	7.43
Total	99.59	99.99	99.04	100.39	100.32	100.37	99.49	100.46	100.42	100.19	100.42	100.39	100.51
Sc	15.5	12.9	13.9	11.4	8.01	15.8	22.4	18.8	17.8	12.9	9.63	10.9	13.9
V	212	141	173	112	103	163	199	160	149	123	93	123	149
Cr	160	133	135	122	115	206	378	156	160	148	113	129	187
Co	18.2	15.7	4.43	3.63	8.50	22.9	11.9	14.1	8.73	12.7	10.1	12.4	6.78
Ni	43	48	34	24	34	101	53	46	29	52	38	51	44
Cu	12	20	<2	3	<2	26	39	13	9	13	5	18	16
Zn	100	79	40	25	44	85	99	66	50	69	61	74	59
As	7.29	14.3	5.69	1.41	1.03	6.00	8.23	1.75	0.83	8.58	10.8	4.17	1.96
Se	0.02	0.05	0.32	0.05	<0.11	0.10	0.16	0.04	<0.15	0.08	0.09	<0.1	<0.13
Br	0.16	0.29	0.27	0.19	0.26	0.21	0.23	0.20	0.23	0.30	0.38	0.20	0.22
Rb	108	83.5	44.4	34.9	34.4	60.6	142	96.6	81.7	61.4	48.4	68.4	76.5
Sr	139	226	32	21	106	145	144	132	116	138	218	270	144
Y	18	15	8	12	16	14	24	10	10	29	10	21	14
Zr	113	100	178	131	111	115	168	91	121	130	112	134	126
Nb	7.0	8.0	15.0	8.0	7.0	8.0	12	8.0	9.0	8.0	7.0	10	9.0
Sb	0.59	0.50	0.43	0.26	0.00	0.36	1.02	0.24	0.15	0.48	0.24	0.42	0.08
Cs	5.95	3.98	3.36	1.81	2.06	4.07	5.61	2.91	2.81	3.01	2.63	2.33	2.89
Ba	806	966	505	1112	393	686	1149	761	642	646	596	478	728
La	19.2	27.9	11.8	19.5	27.1	8.52	30.7	11.4	9.04	50.6	9.24	7.54	13.7
Ce	35.7	61.9	15.3	32.1	42.8	17.0	38.5	22.4	17.5	47.8	20.9	14.4	24.1
Nd	16.9	26.5	7.79	18.0	24.2	8.62	28.5	12.3	10.9	49.3	10.9	7.77	8.29
Sm	3.71	5.03	1.91	3.50	4.41	1.66	5.31	2.05	1.79	8.45	1.99	1.62	2.13
Eu	1.17	1.40	0.57	1.03	1.08	0.57	1.43	0.65	0.57	2.22	0.56	0.47	0.65
Gd	3.10	4.11	1.98	2.61	4.26	1.39	4.75	1.52	1.47	6.53	1.73	0.93	1.45
Tb	0.51	0.66	0.22	0.35	0.56	0.22	0.70	0.29	0.28	0.85	0.24	0.30	0.28
Tm	0.25	0.36	0.23	0.38	0.28	0.32	0.56	0.29	0.30	0.40	0.16	0.42	0.18
Yb	1.91	1.95	0.94	1.45	1.52	1.65	2.60	1.60	1.22	2.20	0.97	1.35	1.30
Lu	0.29	0.28	0.15	0.21	0.19	0.24	0.38	0.23	0.19	0.32	0.14	0.21	0.20
Hf	3.19	3.37	5.16	3.62	2.89	2.75	4.28	2.94	3.23	2.87	2.51	2.15	3.15
Ta	0.21	0.29	0.90	0.29	0.26	0.21	0.50	0.29	0.38	0.33	0.27	0.24	0.26
Ir (ppb)	<3	<2.9	<2.6	<2	1.4	1.6	0.6	<2.9	2.4	0.5	<1.5	<1.9	<2.8
Au (ppb)	9.6	4.9	3.5	5.8	<7.2	5.0	15.6	2.9	3.1	7.3	4.2	2.0	3.2
Th	3.13	3.95	8.33	3.19	2.57	2.76	5.33	2.86	2.74	2.99	2.23	1.93	3.44
U	1.82	1.34	1.96	1.37	0.63	0.62	1.29	0.67	0.76	1.02	0.96	0.58	0.72
CIA	84	74	93	88	81	79	80	82	83	81	69	70	85
K/U	18836	22736	6472	11700	7966	18587	32611	19002	18753	15849	11783	16513	16098
Zr/Hf	35.4	29.7	34.5	36.2	38.4	41.8	39.3	31.0	37.5	45.3	44.6	62.3	40.0
La/Th	6.13	7.06	1.42	6.11	10.54	3.09	5.76	3.99	3.30	16.92	4.14	3.91	3.98
Hf/Ta	15.2	11.6	5.73	12.5	11.1	13.1	8.56	10.1	8.50	8.70	9.30	8.96	12.1
Th/U	1.72	2.95	4.25	2.33	4.08	4.45	4.13	4.27	3.61	2.93	2.32	3.33	4.78
La <sub>N</sub> /Yb <sub>N</sub>	6.79	9.67	8.48	9.09	12.1	3.49	7.98	4.81	5.01	15.5	6.44	3.77	7.12
Gd <sub>N</sub> /Yb <sub>N</sub>	1.32	1.71	1.71	1.46	2.27	0.68	1.48	0.77	0.98	2.41	1.45	0.56	0.90
Eu/Eu*	1.05	0.94	0.90	1.04	0.76	1.15	0.87	1.13	1.07	0.91	0.92	1.17	1.13

<sup>a</sup>Major elements in wt%, trace elements in ppm, except as noted. Total Fe as Fe<sub>2</sub>O<sub>3</sub>. Eu/Eu\* = Eu<sub>N</sub>/(Sm<sub>N</sub> × Gd<sub>N</sub>)<sup>0.5</sup>. Chemical index of alteration (CIA) = (Al<sub>2</sub>O<sub>3</sub>/[Al<sub>2</sub>O<sub>3</sub> + CaO + Na<sub>2</sub>O + K<sub>2</sub>O]) × 100 in molecular proportions.

Table 4. Averages compositions (and standard deviations) of analyzed samples compared to those of target rocks.<sup>a</sup>

	Suevite average	Claystone average	Fragmentary matrix average	Shale average <sup>b</sup>	Graywacke phyllite average <sup>b</sup>	Granite dike average <sup>b</sup>	Pepiakese granite average <sup>b</sup>	Ivory Coast tektites average <sup>b</sup>	Upper continental crust <sup>c</sup>
SiO <sub>2</sub>	63.58 ± 3.01	62.41 ± 5.75	65.36 ± 1.99	55.56	66.75	68.74	57.81	67.58	66.0
TiO <sub>2</sub>	0.64 ± 0.07	0.68 ± 0.12	0.59 ± 0.05	0.84	0.66	0.50	0.46	0.56	0.5
Al <sub>2</sub> O <sub>3</sub>	15.58 ± 1.15	18.33 ± 2.32	16.77 ± 1.06	19.56	15.27	15.91	16.45	16.74	15.2
Fe <sub>2</sub> O <sub>3</sub>	6.58 ± 2.24	6.63 ± 1.84	5.97 ± 0.68	8.54	6.37	3.97	6.09	6.16	4.5
MnO	0.11 ± 0.05	0.06 ± 0.05	0.06 ± 0.01	0.05	0.03	0.01	0.07	0.06	–
MgO	1.43 ± 0.54	1.51 ± 0.66	1.48 ± 0.28	2.90	2.12	1.44	6.63	3.46	2.2
CaO	1.39 ± 0.61	0.21 ± 0.17	0.12 ± 0.12	0.09	0.19	0.31	4.36	1.38	4.2
Na <sub>2</sub> O	1.73 ± 0.53	0.73 ± 0.37	1.92 ± 1.27	1.00	2.26	4.14	6.04	1.90	3.9
K <sub>2</sub> O	1.27 ± 0.38	2.10 ± 0.96	1.82 ± 0.27	2.89	1.80	1.92	0.67	1.95	3.4
P <sub>2</sub> O <sub>5</sub>	0.09 ± 0.03	0.07 ± 0.04	0.05 ± 0.01	0.08	0.06	0.06	0.10	–	–
LOI	7.68 ± 2.22	7.37 ± 1.36	6.24 ± 0.97	7.91	4.25	2.98	1.48	0.002	–
Total	100.10	100.01	100.38	99.41	99.76	99.98	100.15	99.79	–
Sc	15.3 ± 5.3	15.2 ± 4.2	11.8 ± 1.9	23.4	15.5	9.76	17.5	14.7	11
V	120 ± 45	157 ± 36	122 ± 22	184	134	91	110	–	60
Cr	373 ± 615	174 ± 81	144 ± 32	194	165	127	517	244	35
Co	19.9 ± 12.7	12.0 ± 6.4	10.5 ± 2.7	22.6	12.1	9.66	30.4	26.7	10
Ni	106 ± 108	46 ± 22	46 ± 6	79	48	49	172	157	20
Cu	24 ± 21	17 ± 12	13 ± 6	52	16	11	24	–	25
Zn	73 ± 16	65 ± 27	66 ± 7	143	104	82	90	23	71
As	3.10 ± 1.0	5.17 ± 4.47	6.38 ± 4.03	8.61	7.00	14.9	12.7	0.45	1.5
Se	0.10 ± 0.06	0.11 ± 0.11	0.09 ± 0.01	0.19	0.16	0.21	0.09	0.23	50
Br	0.21 ± 0.03	0.23 ± 0.04	0.28 ± 0.08	0.23	0.18	0.15	0.16	0.79	0.79
Rb	51.4 ± 17.7	76.2 ± 36.3	63.7 ± 11.8	104	65.2	69.9	22.4	66	112
Sr	301 ± 56	118 ± 61	193 ± 63	118	152	342	377	260	350
Y	16 ± 2	14 ± 5	18 ± 8	24	19	11	11	–	22
Zr	122 ± 19	125 ± 29	125 ± 9	153	143	129	82	134	190
Nb	8.0 ± 2.6	9.1 ± 2.6	8.5 ± 1.3	6.1	5.7	3.7	1.8	–	25
Sb	0.33 ± 0.16	0.39 ± 0.30	0.31 ± 0.18	0.38	0.20	0.18	0.42	0.23	0.2
Cs	3.71 ± 3.78	3.62 ± 1.44	2.72 ± 0.30	5.57	3.27	4.22	0.87	3.67	3.7
Ba	563 ± 83	780 ± 258	612 ± 104	765	454	605	226	327	550
La	18.9 ± 5.1	18.4 ± 8.6	20.3 ± 20.3	30.9	23.4	18.8	15.6	20.7	30
Ce	38.8 ± 8.5	31.5 ± 15.2	26.8 ± 14.5	38.4	34.8	39.4	32.0	41.9	64
Nd	18.2 ± 4.8	17.1 ± 7.8	19.1 ± 20.1	28.2	26.5	19.8	17.5	21.8	26
Sm	3.53 ± 0.74	3.26 ± 1.45	3.55 ± 3.28	5.48	5.06	3.74	3.58	3.95	4.5
Eu	1.07 ± 0.18	0.94 ± 0.36	0.98 ± 0.83	1.37	1.29	1.03	1.19	1.2	0.88
Gd	2.92 ± 0.95	2.80 ± 1.32	2.66 ± 2.60	6.55	4.80	3.40	3.07	3.34	3.8
Tb	0.47 ± 0.10	0.42 ± 0.19	0.42 ± 0.29	1.06	0.73	0.59	0.47	0.56	0.64
Tm	0.33 ± 0.13	0.33 ± 0.10	0.29 ± 0.14	0.47	0.35	0.22	0.20	0.30	0.33
Yb	1.57 ± 0.28	1.65 ± 0.48	1.46 ± 0.52	2.70	2.14	1.13	1.18	1.79	2.2
Lu	0.23 ± 0.04	0.24 ± 0.07	0.22 ± 0.07	0.38	0.29	0.16	0.14	0.24	0.32
Hf	3.22 ± 0.24	3.49 ± 0.78	2.67 ± 0.43	4.12	4.04	3.66	1.88	3.38	5.8
Ta	0.30 ± 0.08	0.37 ± 0.22	0.28 ± 0.04	0.53	0.42	0.28	0.19	0.34	2.2
W	–	–	0.6	0.5	0.64	0.84	0.54	0.63	2
Ir (ppb)	1.1 ± 0.3	1.5 ± 0.7	0.5	–	–	–	–	–	0.02
Au (ppb)	0.3 ± 10.9	6.3 ± 4.3	4.2 ± 2.2	11.8	10.3	21.5	18.3	56	1.8
Th	2.94 ± 0.61	3.87 ± 1.88	2.65 ± 0.69	4.36	3.94	3.10	2.21	3.54	10.7
U	1.05 ± 0.58	1.16 ± 0.52	0.82 ± 0.21	1.69	1.35	1.75	0.74	0.94	2.8
CIA	70	83	76	80	72	63	47	–	46
K/U	10568	17407	15061	14190	11064	9104	7513	17287	10076
Zr/Hf	37.9	36.0	48.1	37.1	35.4	35.2	43.6	39.6	32.8
La/Th	6.54	5.27	7.24	7.09	5.94	6.06	7.06	5.85	2.8
Hf/Ta	11.6	10.7	9.77	7.77	9.62	13.1	9.89	9.94	2.64
Th/U	3.34	3.53	3.34	2.58	2.92	1.77	2.99	3.77	3.82
La <sub>N</sub> /Yb <sub>N</sub>	8.19	7.49	8.22	7.73	7.39	11.2	8.93	7.81	9.21
Gd <sub>N</sub> /Yb <sub>N</sub>	1.52	1.37	1.33	1.97	1.82	2.44	2.11	–	1.4
Eu/Eu*	1.10	0.99	1.03	0.70	0.80	0.88	1.10	1.01	0.65

<sup>a</sup>Major elements in wt%, trace elements in ppm, except as noted. Total Fe as Fe<sub>2</sub>O<sub>3</sub>. Blank spaces = not determined. Chemical index of alteration (CIA) = (Al<sub>2</sub>O<sub>3</sub>/[Al<sub>2</sub>O<sub>3</sub> + CaO + Na<sub>2</sub>O + K<sub>2</sub>O]) × 100 in molecular proportions. Eu/Eu\* = Eu<sub>N</sub>/(Sm<sub>N</sub> × Gd<sub>N</sub>)<sup>0.5</sup>.

<sup>b</sup>Data from Koeberl et al. (1998).

<sup>c</sup>Data from Taylor and McLennan (1985).

matrix samples; its composition is probably due to extensive chloritization and a significant proportion of amphibole and/or biotite. The sample also contains high Cr, V, Co, and Ni, suggesting a basaltic component. If sample BH1/1000 is removed from the calculation of the average for BH1, the more mafic nature is still retained. The suevite samples show

a composition range that is comparable to the range in target rocks compositions, especially the phyllite-graywacke and granitoids (see Koeberl et al. 1998).

Harker variation diagrams showing the scatter in the major element compositions are displayed in Fig. 6. Apart from the CaO diagram, which clearly separates the suevites

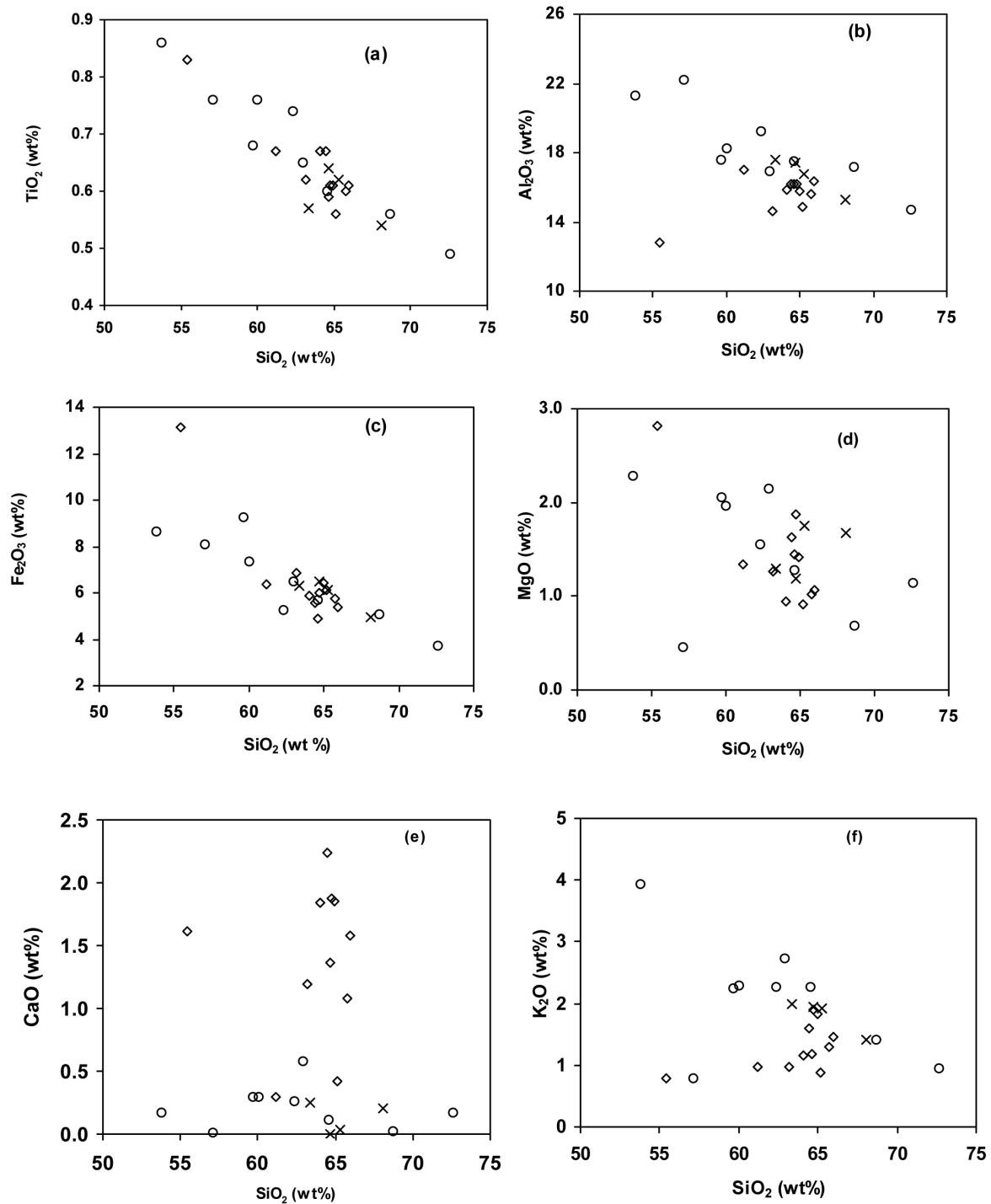


Fig. 6. Harker variation diagrams for the various groups of samples studied. Open diamonds represent suevite; circles represent claystone (highly weathered target rocks); crosses represents fragmentary matrix (micro-lithic breccia).

from the other samples, no clear distinction exists between the different groups of samples. This may be due to the fact that the suevite, fragmentary matrix, and claystone are all derived from similar target rocks and that the high CaO content in the suevite is suggestive of a post-impact carbonate component, as fillings in the voids in the suevites. No correlation between the contents of SiO<sub>2</sub> and CaO is observed. However, significant negative correlations exist, especially in the claystone samples, for SiO<sub>2</sub> with TiO<sub>2</sub>, Fe<sub>2</sub>O<sub>3</sub>, Al<sub>2</sub>O<sub>3</sub>, K<sub>2</sub>O, and MgO.

Figure 7 shows the major element compositions of suevite, fragmentary matrix, and claystone in terms of Al<sub>2</sub>O<sub>3</sub>-(CaO + Na<sub>2</sub>O)-K<sub>2</sub>O and Al<sub>2</sub>O<sub>3</sub>-(CaO + Na<sub>2</sub>O + K<sub>2</sub>O)-(Fe<sub>2</sub>O<sub>3</sub> + MgO) contents (Figs. 7a and 7b) and in terms of CIPW normative mineralogy (Fig. 7c). Figure 7a shows that all the samples analyzed in this study, and even the target or parent rocks, show a marked depletion of K, Na, and Ca compared to the upper continental crust. They plot toward the Al<sub>2</sub>O<sub>3</sub> corner, suggesting that these samples are highly weathered, with the probable exception of the Pepiakese granite. This weathering is noted in the petrographic and field observations. As would be expected, some of the weathered suevite and claystone samples plot very close to the Al<sub>2</sub>O<sub>3</sub> corner. In Fig. 7b, a shift toward the Fe<sub>2</sub>O<sub>3</sub> + MgO apex

suggests significant contribution of mafic components in the samples. Some iron-rich minerals in the form of iron oxides were observed in the samples. Also present are biotite and chlorites that might have contributed the Fe and Mg contents. The CIPW diagram (Fig. 7c) indicates the high content of quartz in the samples compared with upper continental crust. This agrees with the abundance of quartz shown by the XRD analysis. Also, a slight shift toward the plagioclase apex (Ab + An) exists, especially for the suevite, which reflects the significant presence of albite, as also indicated by the XRD analysis.

Fragmentary matrix samples, as well as most of the suevites, have very similar compositions. This strongly suggests that the variety of precursor rocks was limited and that the proportions of the precursor rocks that mixed into the different breccia types must have been similar. We can make use of these diagrams for speculation regarding the precursor rocks for the Bosumtwi suevite and the fragmentary matrix. Figure 7 indicates that graywacke-phyllite and granite dike components are important contributors to the composition of the suevite and fragmentary matrix, and even the tektites, and that, apparently, the contribution of Pepiakese granite was minor. This is in agreement with drill core observations and

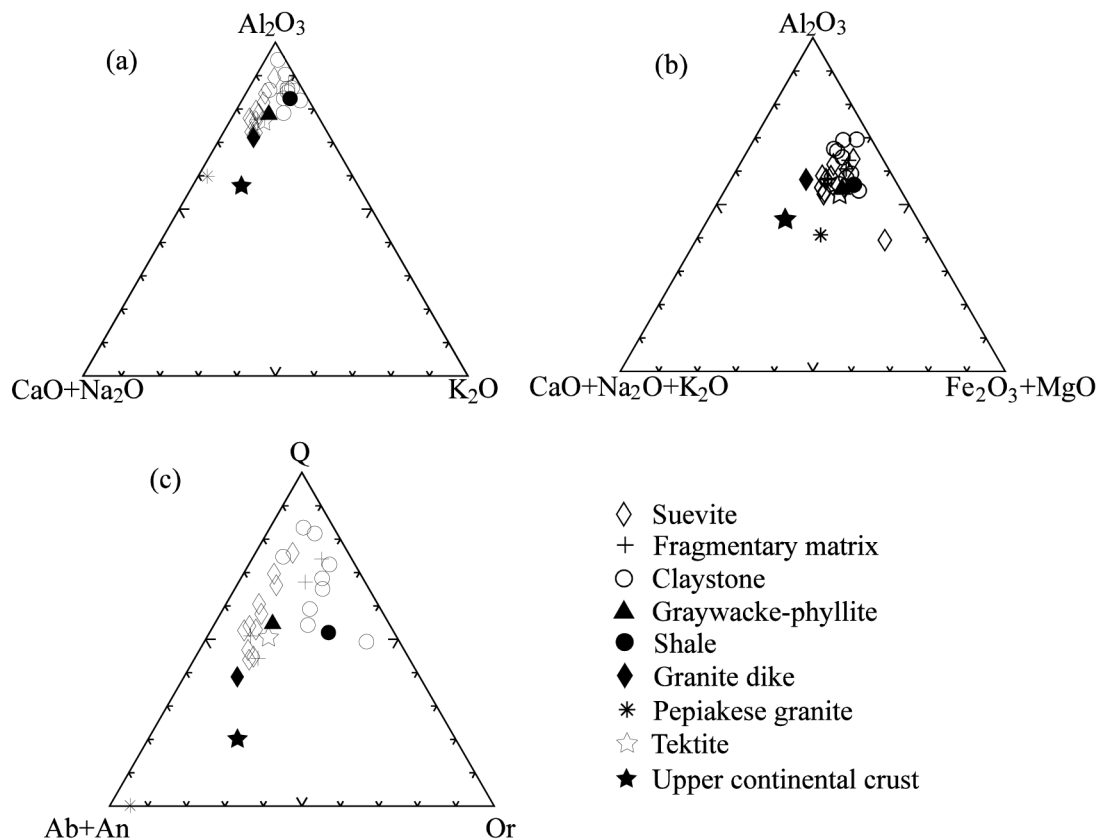


Fig. 7. Major element composition of all samples studied, in terms of (a) Al<sub>2</sub>O<sub>3</sub>-CaO + Na<sub>2</sub>O-K<sub>2</sub>O and (b) Al<sub>2</sub>O<sub>3</sub>-(CaO + Na<sub>2</sub>O + K<sub>2</sub>O)-(Fe<sub>2</sub>O<sub>3</sub> + MgO). Fig. 7c is CIPW normative mineralogy of the samples studied. The average compositions of target rocks, Ivory Coast tektites (Koeberl et al. 1998), and upper continental crust (Taylor and McLennan 1985) are included for comparison.

geological observations (clast population) of various suevite outcrops that show the dominance of graywacke and phyllite. Figure 7c shows that shale is more associated with the claystone than the other groups of samples. Our petrographic observations also confirm that the clast populations identified in different drill cores and in different parts of a given drill core only vary to certain degrees. According to Koeberl et al. (1996), a better prediction for the compositions of the target rocks that formed the suevite can be based on the results of the mixing model calculations. Koeberl et al. (1998) performed mixing calculations to obtain some constraints on the rocks that might have melted to form the Ivory Coast tektites and found a mixture of country rocks that include about 70% graywacke-phyllite, 16% granite dike, and 14% Papiakese granite.

#### *Trace Element Distributions*

Trace element concentrations in the samples show similar trends as those observed for major elements, with restricted range in the suevites and the fragmentary matrix samples compared to the claystone samples. The high Ba, Cs, and Rb contents correlate with high  $K_2O$ , suggesting that these elements are probably incorporated in K-feldspar. Strontium is slightly lower in the more weathered claystone and fragmentary matrix samples compared to the suevite. Its distribution is also similar to the geochemically related Ca. Sample BH2/0950, which has the highest  $Al_2O_3$  content of 22.24 wt%, also has the highest contents for Zr (178 ppm), Nb (15 ppm), Hf (5.16 ppm), Ta (0.90 ppm), Th (8.33 ppm), and U (1.96 ppm) and has a chemical index of alteration (CIA) of 93. This suggests a highly weathered sample with a significant component of granite, with heavy mineral, like zircon. With only one exception (sample BH1/1000), no obvious chemical anomalies were recognized in the suevite and the other samples. This sample has the highest contents of Fe, Mg, Sc, V, Cr, Co, Ni, Cu, Zn. It also has a high content of Au (18.8 ppb) and Ir  $\leq 7$  ppb. The siderophile element data obtained in this study do not readily reveal the presence of an extraterrestrial component in the suevites and the fragmentary matrix. Though sample BH1/1000 has elevated values for Cr (2229 ppm), Co (56.6 ppm), and Ni (423 ppm), the results do not show a statistically significant enrichment compared to the contents observed for the presumed target rocks, especially Papiakese granite (see Koeberl et al. [1998], Table 2a and Jones [1985b], Table 1). However, Dai et al. (in preparation) have performed radiochemical neutron activation analyses and ICP-MS analyses of some samples to determine the contents of the platinum group elements (PGEs) and found enrichments in the impact glasses from the Bosumtwi suevite, which may indicate the presence of a meteoritic component.

For the claystone samples BH4/0450 and BH4/1350 from BH4, a significant variation exists in the concentrations of the various elements with depth. Sample BH4/0450, with a high  $SiO_2$  content of 72.61 wt% as opposed to 59.67 wt% for BH4/1350, has lower concentrations in all the elements apart from Na, Y, Hf, Ta, and REE, which could be associated with

a quartz diluting effect. The higher REE in sample BH4/0450, with a higher  $SiO_2$  content, suggests that REE are not influenced by high quartz in the sample. It is possible that some REE-rich minerals are present in sample BH4/0450. The same situation is observed for the 2 claystone samples from BH2 (BH2/0950 and BH2/1800). The deeper or lower sample (BH2/1800), with a high  $SiO_2$  content, has lower concentrations of all the other elements apart from K, Mg, Ba, and REE.

The absolute abundances of Th and U are highly variable (1.24–8.33 ppm and 0.40–2.59 ppm, respectively). The values of Th/U are also variable (Th/U = 1.31–7.08), but the average Th/U = 3.34, 3.53, and 3.34, respectively, for the suevite, claystone, and the fragmentary matrix are lower than the average of Post-Archean sediments (Th/U =  $5.0 \pm 0.7$ ; Nance and Taylor 1977). They are, however, not very different from the average of 3.8 for upper continental crust (Taylor and McLennan 1985). The slightly lower values of these group of samples probably indicate that oxidation and leaching of uranium has been minimal. The Zr/Hf ratios average 37.9, 36.0, and 48.1, respectively for the suevite, claystone, and the fragmentary matrix, which is not significantly different from the zircon value of 39 (Murali et al. 1983), suggesting the presence of zircon in the samples. The presence of zircon is also supported by the strong correlation between the Zr and Hf contents.

#### *Rare Earth Element (REE) Distributions*

The chondrite-normalized (Taylor and McLennan 1985) REE abundance plots for the suevite samples from the 2 drill cores are shown in Figs. 8a and 8b. The patterns have similar shapes and slopes with general enrichment of light rare earth elements (LREE) and rather flat heavy rare earth elements (HREE). The steep REE patterns, without discernable negative Eu anomalies, are typical of Archean crustal rocks (Taylor and McLennan 1985). The slightly different patterns may be due to the mixture of the various presumed target rocks (graywacke, phyllite, shale, and granitoids) (e.g., Koeberl et al. 1998) at different proportions. The average Eu/Eu\* value for the suevite is about 1.00. A significant positive Eu anomaly of sample BH3/0660 exists (Eu\*/Eu = 2.29), which is commonly attributed to local high concentrations of plagioclase (Nance and Taylor 1977). This may corroborate the significant presence of albite in the suevite analyzed by XRD. With the exception of samples BH1/1000, BH3/0990, and BH3/0220, the suevite has only a limited range in REE abundances. The lower REE contents in sample BH1/1000, with high  $Fe_2O_3$ , MgO, and Cr, could be due to a significant contribution of mafic rocks (see above).

The fragmentary matrix samples also have LREE enrichment and flat HREE patterns (Fig. 9a), with the exception of BD3. The claystone samples have REE patterns (Fig. 9b) similar to those of the suevite, with enrichments in the LREE and a rather flat HREE. The  $La_N/Yb_N$  values range from 3.49 to 12.05, suggesting different mixtures of mafic and

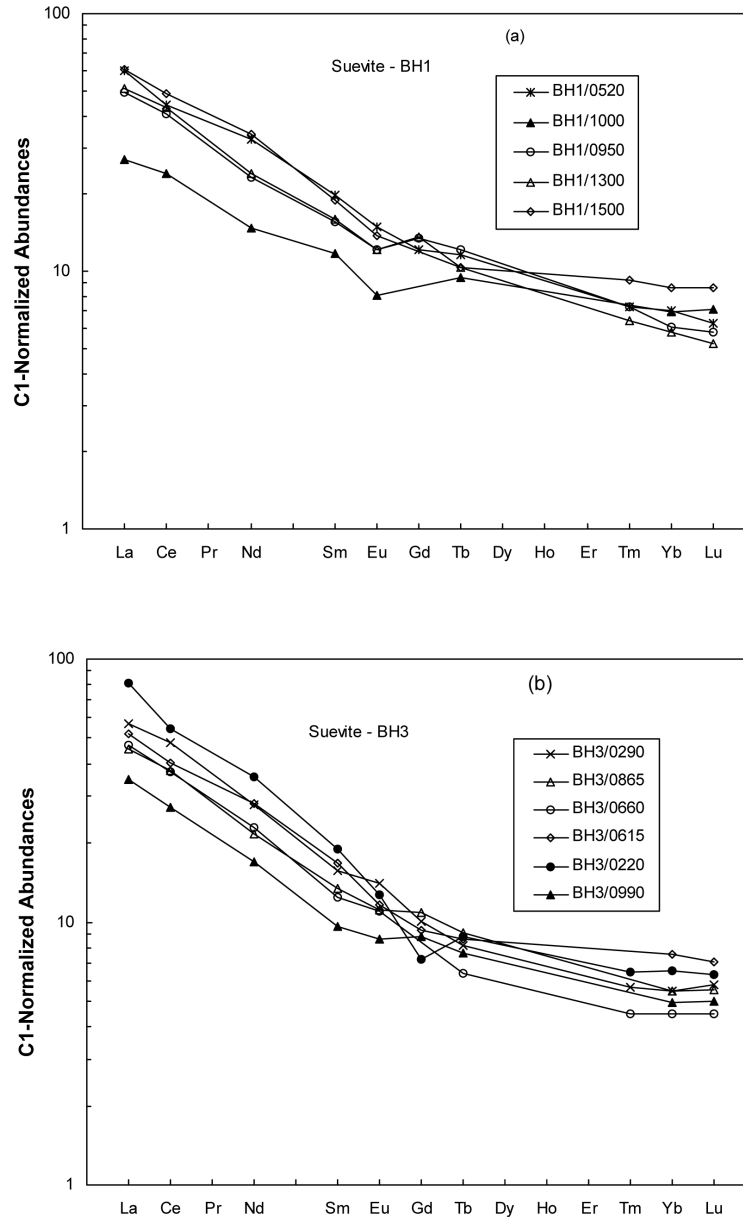


Fig. 8. Chondrite-normalized REE patterns for the suevites from the two drill holes (a) BH1 and (b) BH3. The normalization factors are after Taylor and McLennan (1985).

felsic rocks or REE mobilization and fractionation in these highly weathered samples. According to Nesbitt (1979) and Humphris (1984), the mobilization and fractionation of REE during weathering result from different factors related to the abundance of REE-bearing minerals in the parent rock and the stability of these minerals during weathering.

As for the other trace elements, the REE concentrations of the samples show a limited range, although in detail some important differences exist with and between different lithologies. Figure 10 shows the average REE patterns of the 3 groups of samples investigated. The close similarity in the shape of these average patterns suggests that the origin of the REE-containing fraction of these rocks was essentially the

same throughout the time-span reflected by the different groups of samples. It also suggests that the REE patterns are not significantly influenced by weathering or the impact event, or no obvious REE mobilization and fractionation occurs during these processes. This also seems to support the earlier observations from the major elements that the samples are from a common source. Chondrite-normalized REE patterns for the averages of the various groups of samples studied, together with those of the target rocks and tektites (Koeberl et al. 1998) are shown in Fig. 11. No significant difference exists in the patterns, supporting the suggestions that the various groups of samples studied, and the tektite, were formed from the same target rocks mixed at different proportions.

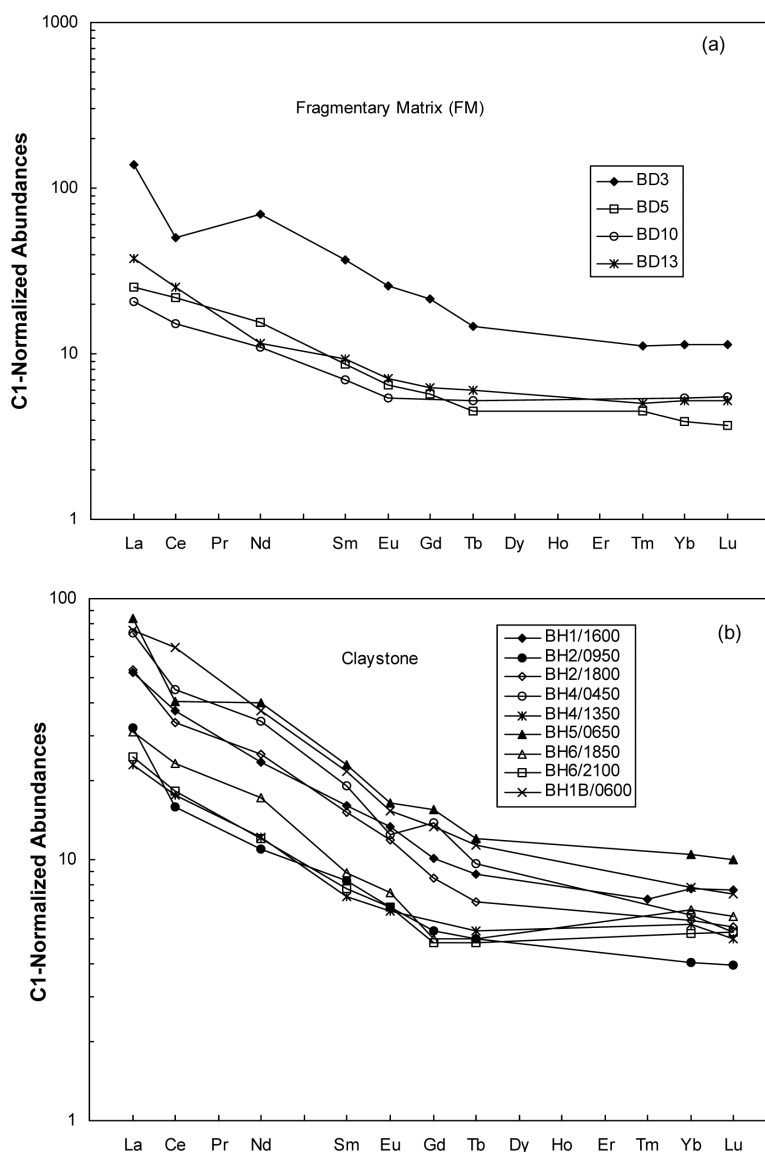


Fig. 9. Chondrite-normalized REE patterns for (a) fragmentary matrix and (b) claystone (highly weathered target rocks). The normalization factors are after Taylor and McLennan (1985).

### Comparison with the Suevite Distribution at the Ries Crater

The present-day suevite distribution is likely to be caused by differential erosion and does not reflect the initial areal extent of the continuous Bosumtwi ejecta deposits. Because fallout suevite thickness ranges from a few meters to only tens of meters, most of the suevite may have been eroded in this tropical environment, where weathering can be as deep as 50 m. Also, larger areas, possibly, were originally covered by a thin veil of suevite that was later eroded. On the other hand, the suevite ejecta plume could have been irregular and discontinuous (depending on the impact angle; cf., Artemieva 2002), which resulted in a discontinuous distribution pattern of the fallout suevite.

The spatial distribution of the Bosumtwi suevite is comparable to the well-studied Ries crater in Germany, which is about twice the size of Bosumtwi and where the fallout suevite occurs in patches of 10 to 20 m thickness and up to 500 m in lateral extent (Hörz 1982). The maximum volume of suevite deposited beyond the crater rim to the north is estimated at  $<0.02 \text{ km}^3$ . The composition of  $\sim 70 \text{ vol}\%$  groundmass or fine-grained matrix and  $\sim 15 \text{ vol}\%$  impact glass of the Bosumtwi suevite outside of the crater rim to the north is also comparable to 75 to 85% and an average of  $\sim 15\%$ , respectively, at Ries (Hörz 1982); this has recently been quantified by Koeberl et al. (2002) in a high-resolution X-ray computed tomography study. The Bosumtwi glasses also display signs of recrystallization (feldspar, pyroxene, and montmorillonite) similar to those at the Ries (Hörz 1982; Engelhardt et al. 1995).

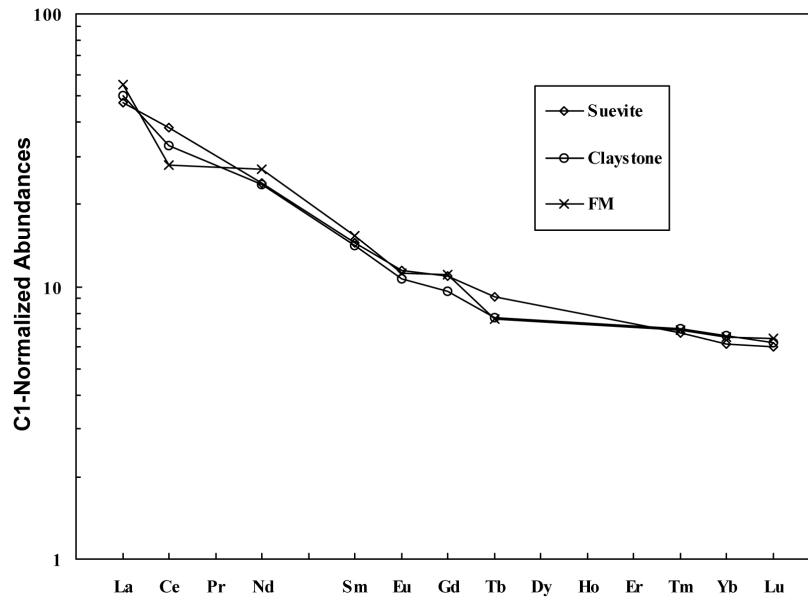


Fig. 10. Chondrite-normalized REE patterns for the averages of the various groups of samples studied. The normalization factors are after Taylor and McLennan (1985).

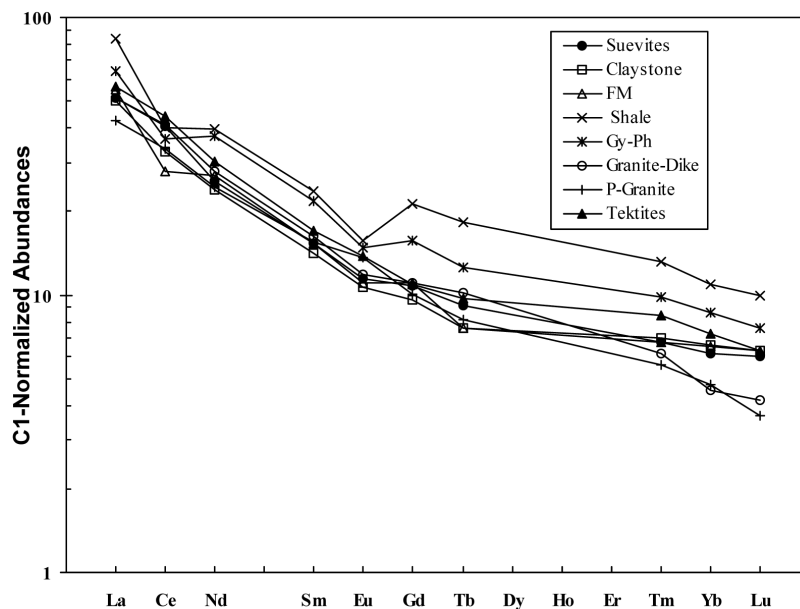


Fig. 11. Chondrite-normalized REE patterns for the averages of the various groups of samples studied together with those of target rocks and tektites (Koeberl et al. 1998). The normalization factors are after Taylor and McLennan (1985).

Kieffer and Simonds (1980) postulated that impacts into sediments rich in volatiles (e.g.,  $H_2O$ ,  $CO_2$ ) will result in significantly larger volumes of impact-generated vapor phases when compared to impacts into purely crystalline (volatile-poor) terranes. The form and amount of impact melts generated in both cases may be dramatically affected by the vapor phase: little interaction in the “anhydrous” crystalline terrane results in coherent melt sheets (e.g., Brent, Clearwater, and Manicouagan craters; Grieve 1980), while abundant vapor phases in sedimentary targets will disrupt the

melt to form discrete bombs (Hörz 1982). This seems to apply to the Bosumtwi suevite, where the melt is in the form of bombs, though the target rocks are mixed granitic basement with overlying sedimentary rocks.

### Meteoritic Component

Due to low contents of Ir and the limit of detection of the INAA method, an extraterrestrial (meteoritic) component in the breccias cannot be identified unambiguously. Deep

drilling underneath the crater lake (which is planned for 2004) will be necessary to identify a melt sheet that may preserve a meteoritic component. However, a meteoritic component has been found in the Ivory Coast tektites and some impact glasses derived from the Bosumtwi impact (cf., Koeberl and Shirey 1993).

### SUMMARY AND CONCLUSIONS

Until now, no integrated petrographical, mineralogical, and geochemical studies of drill core data and breccias from the Bosumtwi impact structure had been available; thus, we studied 11 suevite samples from 2 drill holes, 9 claystone (highly weathered target rocks) samples from 6 drill holes just outside the northern part of the crater rim, and 4 fragmentary matrix samples (micro-lithic breccia) from road cuts. Our main observations and conclusions are summarized in the following paragraphs:

1. The ejecta blanket in the form of suevite covers an area of about 1.5 km<sup>2</sup> in the northern part of the crater, outside the crater rim. The maximum thickness of the suevite was determined to be ~15 m.
2. Depending on the rock types, core recovery ranged from close to 80% in the suevites to 10% or less in the lithic breccias and weathered rocks.
3. Macroscopic studies of the recovered suevite cores show that melt inclusions are present throughout the whole length of the suevite cores in the form of mainly vesicular glasses, with no significant change in character or relative amount with depth. Individual glassy fragments are irregular in shape and some show flowing bands. In general, the groundmass or matrix occupies ~75 vol% of the suevite, ~15 vol% of the glass fragments, ~10 vol% of the rock fragments (greywacke, phyllite, shale, schist and granite), and less than 1 vol% of mineral clasts (quartz and feldspar). The fragments are up to a size greater than the diameter of the core (5 cm). Most fragments are less than 20 mm in diameter. Because the vertical sections of the suevite revealed no primary variation in composition or grain size, the process of deposition is assumed to have been uniform and of short duration.
4. Distinctive shock metamorphic effects at Bosumtwi have so far been found only in the preserved suevite deposits, which occur outside of the crater rim and which represent ejecta from the lower part of the crater. These shock effects include planar deformation features (PDFs) in quartz and feldspar, biotite grains with kinked bands, diaplectic quartz and feldspar glasses, lechatelierite, "ballen"-structured quartz, and shock fused rocks. None of the other (lithic) breccias of probable impact origin (fractured and shattered metasediments and granites) display definite shock effects.
5. The main mineralogical components in the matrix of the samples are quartz, with albite, montmorillonite, mixed-layer clays of illite-smectite type, and variable amounts of kaolinite, chlorite and muscovite. Kaolinite is also present in the highly-weathered samples.
6. Major and trace element analyses of the 24 samples yielded compositions similar to the target rocks in the area (graywacke-phyllite, shale, and granite). Graywacke-phyllite and granite dike seem to be important contributors to the composition of the suevite and the fragmentary matrix, with a minor contribution of Papiakese granite. This is in agreement with drill core and geological observations (clast population) of various outcrops that show only minor shale.
7. The REE patterns show enrichment in light rare earth elements (LREE) with steep slopes and no discernible Eu\*/Eu anomaly, which is typical of Archean crustal rocks. The close similarity in the shape of the average group patterns suggests that the origin of the REE-containing fraction of these rocks was essentially the same in the different group of samples. It also suggests that the REE patterns are not significantly influenced by weathering or the impact event, or no obvious REE mobilization and fractionation occurs during these processes. This also seems to support the observations from the major elements that the samples are from a common source.
8. No significant difference exists in the trace element contents and the chondrite-normalized REE patterns for the groups of samples studied and the target rocks and the tektites, supporting the suggestion that the various groups of samples studied, and the tektites, were formed from the target rocks mixed at different proportions.

*Acknowledgments*—The authors thank the Geological Survey Department of Ghana, especially the Director at the time, Mr. C. E. Oduro, for field and logistic support. D. Boamah thanks the Austrian Academic Exchange Service (ÖAD) for a Ph.D. scholarship and partial financial support for field work. The authors are grateful to W. U. Reimold (University of Witwatersrand, Johannesburg) for his help with the XRF analyses. We are also grateful to Dr. Bevan French for a detailed review of a draft of this manuscript and to journal reviewers S. R. Taylor and P. Claeys for helpful comments. The work was supported by the Austrian Fonds zur Förderung der wissenschaftlichen Forschung, project Y58-GEO (to C. Koeberl).

*Editorial Handling*— Dr. Richard Grieve

### REFERENCES

- Artemieva N. 2002. Tektite origin in oblique impacts: Numerical modeling of the initial stage. In *Meteorite impacts in Precambrian shields*, edited by Plado J. and Pesonen L. J. Impact Studies, vol. 2, Heidelberg: Springer. pp. 257–276.
- Boamah D. and Koeberl C. 1999. Shallow drilling around the

- Bosumtwi crater, Ghana: Preliminary results (abstract). *Meteoritics & Planetary Science* 34:A13–A14.
- Boamah D. and Koeberl C. 2002. Geochemistry of soils from the Bosumtwi impact structure, Ghana, and relationship to radiometric airborne geophysical data. In *Meteorite impacts in Precambrian shields*, edited by Plado J. and Pesonen L. J. Impact Studies, vol. 2, Heidelberg: Springer. pp. 211–255.
- Carstens H. 1975. Thermal history of impact melt rocks in the Fennoscandian Shield. *Contributions to Mineralogy and Petrology* 50:145–155.
- Chao E. C. T. 1968. Pressure and temperature histories of impact metamorphosed rocks—Based on petrographic observations. *Neues Jahrbuch für Mineralogie—Abhandlungen* 108:209–246.
- El Goresy A. 1966. Metallic spherules in Bosumtwi crater glasses. *Earth and Planetary Science Letters* 1:23–24.
- El Goresy A., Fechtig H., and Ottemann T. 1968. The opaque minerals in impactite glasses. In *Shock metamorphism of natural materials*, edited by French B. M. and Short N. M. Baltimore: Mono Book Corporation. pp. 531–554.
- Engelhardt W. V. 1972. Shock produced rock glass from the Ries crater. *Contributions to Mineralogy and Petrology* 36:265–292.
- Engelhardt W. V., Arndt J., Fecker B., and Pankau H. G. 1995. Suvite breccia from the Ries crater, Germany: Origin, cooling history, and devitrification of impact glasses. *Meteoritics* 30: 279–293.
- French B. M. 1998. Traces of catastrophe: A handbook of shock-metamorphic effects in terrestrial meteorite impact structures. *LPI Contribution No. 954*. Houston: Lunar and Planetary Institute. 120 p.
- Garvin J. B., Schnetzler C. C., and Grieve R. A. F. 1992. Characteristics of large terrestrial impact structures as revealed by remote sensing studies. *Tectonophysics* 216:45–62.
- Gibbs A. K., Montgomery C. W., O'Day P. A., and Erslev E. A. 1986. The Archean-Proterozoic transition: Evidence from the geochemistry of metasedimentary rocks of Guyana and Montana. *Geochimica et Cosmochimica Acta* 50:2125–2141.
- Glass B. P. 1968. Glassy objects (microtektites?) from deep sea sediments near the Ivory Coast. *Science* 161:891–893.
- Glass B. P. 1969. Chemical composition of Ivory Coast microtektites. *Geochimica et Cosmochimica Acta* 33:1135–1147.
- Govindaraju K. 1989. 1989 compilation of working values and sample description for 272 geostandards. *Geostandards Newsletter* 13:1–113.
- Grieve R. A. F. 1980. Cratering in the lunar highlands: Some problems with the process, record, and effects. In *Proceedings of the conference on the lunar highlands crust*, edited by Papike J. J. and Merrill R. B. New York: Pergamon Press. pp. 173–196.
- Grieve R. A. F., Dence M. R., and Robertson P. B. 1977. Cratering processes: As interpreted from the occurrence of impact melts. In *Impact and explosion cratering*, edited by Roddy D. J., Pepin R. O., and Merrill R. B. New York: Pergamon Press. pp. 791–814.
- Hirdes W., Davis D. W., and Eisenlohr B. N. 1992. Reassessment of Proterozoic granitoid ages in Ghana on the basis of U/Pb zircon and monazite dating. *Precambrian Research* 56:89–96.
- Hörz F. 1982. Ejecta of the Ries crater, Germany. In *Geological implications of impacts of large asteroids and comets on the earth*, edited by Silver L. T. and Schultz P. H. Boulder: Geological Society of America. Special Paper 190. pp. 39–55.
- Humphris S. E. 1984. The mobility of the rare earth elements in the crust. In *Rare earth element geochemistry*, edited by Henderson P. New York: Elsevier. pp. 317–340.
- Jones W. B. 1985a. The origin of the Bosumtwi crater, Ghana—An historic review. *Proceedings of the Geological Association (London)* 96:275–284.
- Jones W. B. 1985b. Chemical analyses of Bosumtwi crater target rocks compared with Ivory Coast tektites. *Geochimica et Cosmochimica Acta* 49:2569–2576.
- Jones W. B., Bacon M., and Hastings D. A. 1981. The Lake Bosumtwi impact crater, Ghana. *Geological Society of America Bulletin* 92:342–349.
- Junner N. R. 1937. The geology of the Bosumtwi caldera and surrounding country. *Gold Coast Geological Survey Bulletin* 8: 1–38.
- Kieffer S. W. and Simonds C. H. 1980. The role of volatiles and lithology in the impact cratering process. *Reviews of Geophysics and Space Physics* 18:143–181.
- Koeberl C. 1993. Instrumental neutron activation analysis of geochemical and cosmochemical samples: A fast and proven method for small sample analysis. *Journal of Radioanalytical and Nuclear Chemistry* 168:47–60.
- Koeberl C. 1994. African meteorite impact craters: Characteristics and geological importance. *Journal of African Earth Sciences* 18:263–295.
- Koeberl C. 1997. Impact cratering: The mineralogical and geochemical evidence. In *Ames structure in northwest Oklahoma and similar features: Origin and petroleum production (1995 symposium)*, edited by Johnson K. S. and Campbell J. A. *Oklahoma Geological Survey Circular* 100:30–54.
- Koeberl C., Reimold W. U., Kracher A., Träxler B., Vormaijer A., and Körner W. 1996. Mineralogical, petrological, and geochemical studies of drill cores from the Manson impact structure, Iowa. In *The Manson impact structure, Iowa: Anatomy of an impact crater*, edited by Koeberl C. and Anderson R. R. Boulder: Geological Society of America. Special Paper 302. pp. 145–219.
- Koeberl C., Bottomley R. J., Glass B. P., and Storzer D. 1997a. Geochemistry and age of Ivory Coast tektites and microtektites. *Geochimica et Cosmochimica Acta* 61:1745–1772.
- Koeberl C., Reimold W. U., Pesonen L. J., and Brandt D. 1997b. New Studies of the Bosumtwi impact structure, Ghana: The 1997 Field Season (abstract). *Meteoritics & Planetary Science* 32:A72–A73.
- Koeberl C., Reimold W. U., Blum J. D., and Chamberlain C. P. 1998. Petrology and geochemistry of target rocks from the Bosumtwi impact structure, Ghana, and comparison with Ivory Coast tektites. *Geochimica et Cosmochimica Acta* 62:2179–2196.
- Koeberl C., Denison C., Ketcham R. A., and Reimold W. U. 2002. High-resolution X-ray computed tomography of impactites. *Journal of Geophysical Research* 107, doi: 10.1029/2001JE001833.
- Kolbe P., Pinson W. H., Saul J. M., and Miller E. W. 1967. Rb-Sr study on country rocks of the Bosumtwi crater, Ghana. *Geochimica et Cosmochimica Acta* 31:869–875.
- Lacroix A. 1934. Sur la découverte de tectites à la Côte d'Ivoire. *Comptes Rendus des Seances de l'Academie des Sciences de Paris* 199:1539–1542.
- Leube A., Hirdes W., Mauer R., and Kesse G. O. 1990. The early Proterozoic Birimian Supergroup of Ghana and some aspects of its associated gold mineralization. *Precambrian Research* 46: 139–165.
- Littler J., Fahey J. J., Dietz R. S., and Chao E. C. T. 1961. Coesite from the Lake Bosumtwi crater, Ashanti, Ghana (abstract). Geological Society of America Special Paper 68. pp. 218.
- Master S. and Reimold W. U. 2000. The impact cratering record of Africa: An updated inventory of proven, probable, possible, and discredited impact structures on the African continent. In *Catastrophic events and mass extinctions: Impacts and beyond*. LPI Contribution No. 1053. Houston: Lunar and Planetary Institute. pp. 133–134.
- Moon P. A. and Mason D. 1967. The geology of 1/4° field sheets 129 and 131, Bompata S. W. and N. W. *Ghana Geological Survey Bulletin* 31:1–51.

- Murali A. V., Parthasarathy R., Mahadevan T. M., and Sankar Das M. 1983. Trace element characteristics, REE patterns, and partition coefficients of zircons from different geological environments—A case study on Indian zircons. *Geochimica et Cosmochimica Acta* 47:2047–2052.
- Nance W. B. and Taylor S. R. 1977. Rare earth element patterns and crustal evolution—II. Archean sedimentary rocks from Kalgoorlie, Australia. *Geochimica et Cosmochimica Acta* 41: 225–231.
- Nesbitt H. W. 1979. Mobility and fractionation of rare earth elements during weathering of a granodiorite. *Nature* 279:206–210.
- Ojamo H., Pesonen L. J., Elo S., Hautaniemi H., Koeberl C., Reimold W. U., and Plado J. 1997. The Bosumtwi impact structure, Ghana: International geophysical co-operation at the best (abstract). In *Sovelletun geofysiikan XI neuvottelupäivät*, edited by Kaikkonen P., Komminaho K., and Salmirinne H. Oulu: Oulun yliopisto. pp. 10–11.
- Pesonen L. J., Koeberl C., Ojamo H., Hautaniemi H., Elo S., and Plado J. 1998. Aerogeophysical studies of the Bosumtwi impact structure, Ghana (abstract). *Geological Society of America Abstracts with Programs* 30(7):A190
- Pesonen L. J., Plado J., Koeberl C., and Elo S. 1999. The Lake Bosumtwi meteorite impact structure, Ghana: Magnetic modeling (abstract). *Meteoritics & Planetary Science* 34:A91–A92.
- Plado J., Pesonen L. J., Koeberl C., and Elo S. 2000. The Bosumtwi meteorite impact structure, Ghana: A magnetic model. *Meteoritics & Planetary Science* 35:723–732.
- Pohl J., Stöffler D., Gall H., and Ernstson K. 1977. The Ries impact crater. In *Impact and explosion cratering*, edited by Roddy D. J., Pepin R. O., and Merrill R. B. New York: Pergamon Press. pp. 343–404.
- Reimold W. U., Koeberl C., and Bishop J. 1994. Roter Kamm impact crater, Namibia: Geochemistry of basement rocks and breccias. *Geochimica et Cosmochimica Acta* 58:2689–2710.
- Reimold W. U., Brandt D., and Koeberl C. 1998. Detailed structural analysis of the rim of a large, complex impact crater: Bosumtwi crater, Ghana. *Geology* 26:543–546.
- Scholz C. A., Karp T., Brooks K. M., Milkereit B., Amoako P. Y. O., and Arko J. A. 2002. Pronounced central uplift identified in the Bosumtwi impact structure, Ghana, using multichannel seismic reflection data. *Geology* 30:939–942.
- Stöffler D. and Grieve R. A. F. 1994. Classification and nomenclature of impact metamorphic rocks: A proposal to the IUGS subcommission on the systematics of metamorphic rocks. In *ESF Scientific Network on impact cratering and evolution of planet Earth, Post-Östersund Newsletter*, edited by Montanari A. and Smit J. pp. 9–15.
- Stöffler D. and Langenhorst F. 1994. Shock metamorphism of quartz in nature and experiment: I. Basic observation and theory. *Meteoritics* 29:155–181.
- Taylor S. R. and McLennan S. M. 1985. *The continental crust: Its composition and evolution*. Oxford: Blackwell Scientific Publications. 312 p.
- Taylor P. N., Moorbath S., Leube A., and Hirdes W. 1992. Early Proterozoic crustal evolution in the Birimian of Ghana: Constraints from geochronology and isotope geochemistry. *Precambrian Research* 56:97–111.
- Wagner R., Reimold W. U., and Brandt D. 2002. Bosumtwi impact crater, Ghana: A remote sensing investigation. In *Meteorite impacts in Precambrian shields*, edited by Plado J. and Pesonen L. J. Impact Studies, vol. 2. Heidelberg: Springer. pp. 189–210.
- Woodfield P. D. 1966. The geology of the ¼° field sheet 91, Fumso N. W. *Ghana Geological Survey Bulletin* 30:1–66.
- Wright J. B., Hastings D. A., Jones W. B., and Williams H. R. 1985. *Geology and mineral resources of West Africa*. London: Allen & Unwin. 187 p.

## APPENDIX

Table A1. Drill core stratigraphy of suevite-bearing cores.

Depth	Petrographic description
	BH1
0.0–1.5 m	Brownish silty clay.
1.5–3.0 m	Sludge—loose or crumbled suevite, gray in color.
3.0–3.5 m	42% core recovery—21 cm of suevite, gray in color, medium grained and containing about 5 vol% rock clasts up to 20 mm in size made up of graywacke, phyllite, slate, granite, some quartz and feldspar, and about 10 vol% of glass fragments.
3.5–4.0 m	54% core recovery—27 cm broken pieces of suevite similar to above, but with the rock fragments up to about 45 mm in size and about 10 vol% glass fragments.
4.0–5.0 m	About 15% core recovery—Broken pieces of suevite, medium to coarse grained and grayish in color with some dark brown materials (iron oxide?) in some of the broken faces. Glass fragments about 10 vol%, rock fragments about 10 vol%, and mainly graywacke, with some granite. Quartz and feldspar clasts are also present.
5.0–5.5 m	About 38% core recovery—Broken pieces of suevite with 2 large fragments of glass melt, about 50 mm in size. Grayish in color with dark brown materials in the broken faces. Glass fragments about 40 vol% of the recovered core. Rock fragments about 10 vol% and made up of graywacke, shale, and granite. Quartz and feldspar also present.
5.5–6.0 m	100% core recovery—Suevite similar to above with rock fragments (20 vol%).
6.0–6.5 m	100% core recovery—Suevite with about 20 vol% rock fragments of graywacke and granite. Dark brown materials in cracks around 6.04 m. Glass fragments about 10 vol%.
6.5–7.0 m	About 32% core recovery—Suevite with about 20 vol% fragments of glass. Large clast of a fine-grained greenish rock (graywacke) and some clasts of light colored rocks (granite). Rock fragments about 5 vol%.
7.0–7.5 m	About 82% core recovery—Suevite with about 5 vol% rock fragments, mainly graywacke and phyllite, with small amount of granite (smaller sizes). Quartz and feldspar present in small sizes. Glass fragments about 10 vol%. Some dark brown materials (iron oxide) present in cracks at 7.2 m.
7.5–8.0 m	80% core recovery—Suevite with abundant glass clasts (about 40 vol%) and a large fragment of graywacke (70 mm in size). Granite and some quartz and feldspar present in smaller sizes. Rock fragments about 10 vol%.

Table A1. Drill core stratigraphy of suevite-bearing cores. *Continued.*

Depth	Petrographic description
8.0–9.5 m	About 15% core recovery—22 cm of suevite with about 40 vol% of rock fragments and 10 vol% glass fragments. Rocks mostly graywacke with a little granite.
9.5–10.0 m	82% core recovery—Suevite with a lot of glass clasts (about 30 vol%). Rock fragments about 5 vol% mostly graywacke with a size up to 20 mm. Some brownish materials are found in the cracks and breaks. A yellowish porous rock (weathered dolerite?) occurs around 9.95–10 m.
10.0–10.5 m	84% core recovery—Suevite similar to above (about 30 vol% glass fragments). Quartz grains occur in a crack or break at 10.4 m. Rock fragments, mostly graywacke and granite/feldspar, constitutes about 20 vol% of the core.
10.5–11.0 m	90% core recovery—Suevite similar to above. A transparent colorless mineral (quartz glass?) occurs at 10.8 m.
11.0–11.5 m	100% core recovery—Suevite similar to above with about 35 vol% glass fragments. A large fragment of graywacke (about 80 mm in size) occurs around 11.3 m.
11.5–12.0 m	84% core recovery—Suevite with about 25 vol% glass fragments clasts. Rock fragments (about 20 vol%) up to about 30 mm and made up of graywacke, phyllite, and granite. Quartz and feldspar present in small sizes. Brownish materials occur in the fractures in the suevite around 11.7 m and 11.8 m.
12.0–12.5 m	80% core recovery—Suevite with about 25 vol% glass fragments. Rock fragments (about 30 vol%) of mostly graywacke, phyllite, and granite up to 60 mm in size. Most of the melt have formed flow structures. Dark brown materials occur in the cracks in the suevite.
12.5–13.0 m	56% core recovery—Suevite with about 25 vol% of glass fragments. A 30 mm clast of granite with quartz grains occur around 12.6 m. The rock clasts (about 20 vol%) are dominated by graywacke, with a size up to about 40 mm.
13.0–13.5 m	80% core recovery—Suevite with about 20 vol% of glass fragments. A large fragment of graywacke (about 65 mm in size) occurs around 13.2 m. The rock clasts (about 30 vol%) are made up of graywacke, phyllite and granite. A spotted rock (phyllite?), black with light colored feldspar occurs around 13.3 m.
13.5–14.0 m	76% core recovery—Suevite with less porous materials compared to those above. Glass fragments clasts constitute about 20 vol% of core. Rock clasts (about 20 vol%) are made up of phyllite, granite, and graywacke up to about 45 mm in size. Quartz and feldspar are present in smaller sizes.
14.0–14.5 m	92% core recovery— Suevite with a lot of whitish materials compared to those above and with less glass fragments (about 5 vol%). Rock clasts (about 20 vol%) up to 60 mm in size are made up of phyllite, graywacke, and some granite. Glassy quartz occurs around 14.2 m.
14.5–15.0 m	100% core recovery—Suevite similar to above with about 2 vol% of glass fragments.
15.0–16.0 m	22% core recovery—Broken pieces of shale and phyllite with clay (brecciated rock).
16.0–17.0 m	18% core recovery—Highly weathered graywacke and granite (clay) with some quartz grains.
17.0–18.0 m	16% core recovery—Highly weathered graywacke and granite (clay) with some pebbles.
18.0–19.0 m	About 16% core recovery—Weathered graywacke.
	BH3
0.0–2.0 m	No core recovered—Sludge (silty clay).
2.0–2.5 m	84% core recovery—Suevite, porous with some vesicles, grayish in color. Glass fragmentst about 15 vol%. Rock clasts (about 30 vol%) are made up of phyllite, graywacke, and granite up to 30 mm in size. Brownish materials (oxides) found in the fractures and breaks in the suevite.
2.5–3.0 m	96% core recovery— Suevite similar to above but with higher glass clasts (about 30 vol%). Rock clasts (about 15 vol%) mostly graywacke, phyllite, and granite up to about 35 mm in size.
3.0–3.5 m	74% core recovery—Suevite similar to above with about 25 vol% glass clasts. Some of the melt shows flow band. Rock clasts form about 20 vol%, mostly graywacke, phyllite, and granite up to 30 mm. A clast of graywacke is about 80 mm. Some brownish materials and some light rock clasts are found in the cracks.
3.5–4.0 m	75% core recovery—Suevite with about 20 vol% of glass clasts. Rock clasts (about 20 vol%) made up of graywacke, phyllite, and granite up to 40 mm in size. A yellowish-green clast (about 28 mm) is found around 3.95 m.
4.0–4.5 m	52% core recovery—Suevite with about 25 vol% of glass fragments. Rock clasts (about 15 vol%) made up of graywacke, phyllite, and granite up to 40 mm in size.
4.5–5.0 m	84% core recovery—Suevite similar to above but the rock clasts about 25 vol%.
5.0–5.5 m	82% core recovery—Suevite with about 25 vol% glass and rock clasts about 15 vol%.
5.5–6.0 m	78% core recovery—Suevite, grayish in color with glass fragments occupying about 30 vol% and the rock clasts about 10 vol%, made up of graywacke, phyllite, shale, and granite. A large clast of granite (about 60 mm in size) occurs at 5.8 m.
6.0–6.5 m	74% core recovery—Suevite, gray in color and porous. It contains about 25 vol% of glass clasts. Rock clasts (about 10 vol%) are made up of phyllite, granite, graywacke, and shale up to 40 mm in size. Quartz and feldspar are present in smaller clasts.
6.5–7.0 m	78% core recovery— Suevite similar to above with the melts mostly vesicular and showing flow band.
7.0–7.5 m	88% core recovery—Suevite, porous and grayish in color and with abundant glass clasts (about 35 vol%). Vesiculated with flow bands. Rock clasts constitute about 10 vol% made up of granite, graywacke, and phyllite up to 35 mm in size.
7.5–8.0 m	100% core recovery—Suevite with about 20 vol% glass clasts. Rock clasts made up of graywacke, granite, and phyllite constitute about 15 vol%.
8.0–8.5 m	90% core recovery—Suevite with about 15 vol% glass clasts. Rock clasts (about 40 vol%) made up of phyllite, granite, and graywacke. A large clast of phyllite, about 90 mm in size, occurs around 8.3 m. Some whitish spots (feldspars) are present in the suevite.

Table A1. Drill core stratigraphy of suevite-bearing cores. *Continued.*

Depth	Petrographic description
8.5–9.0 m	94% core recovery—Suevite with about 15 vol% glass clasts. Rock clasts (about 10 vol%) made up of phyllite and graywacke up to 55 mm. Whitish spots (feldspar) and quartz present.
9.0–9.5 m	52% core recovery—Suevite with about 60 vol% glass and showing flow structure. Rock clasts constitute about 5 vol%.
9.5–10.0 m	40% core recovery—Suevite with about 25 vol% rock clasts made up of phyllite, graywacke, granite, and shale. Glass clasts constitute about 20 vol%.
10.0–13.0 m	No core recovery—Sludge (silty clay).
13.0–13.5 m	About 24% core recovery—Pieces of weathered graywacke and phyllite, fine- to medium-grained and grayish in color. Brownish clay present.
13.5–14.0 m	About 40% core recovery—Two pieces of graywacke. Fine- to medium-grained and grayish in color. Brownish materials in the cracks and breaks.
14.0–15.0 m	About 26% core recovery—Pieces of graywacke similar to above.
15.0–16.0 m	About 24% core recovery—Weathered phyllite, grayish in color and showing signs of foliation planes.